KERNFORSCHUNGSANLAGE JÜLICH GmbH

Institut für Reaktorwerkstoffe

Graphitic Matrix Materials for Spherical HTR Fuel Elements

Results of Material Development and Irradiation Testing

Catalogue of Pictures and Tables

by

R.-E. Schulze
H. A. Schulze
W. Rind

Jül - Spez - 167
Juli 1982
ISSN 0343-7639

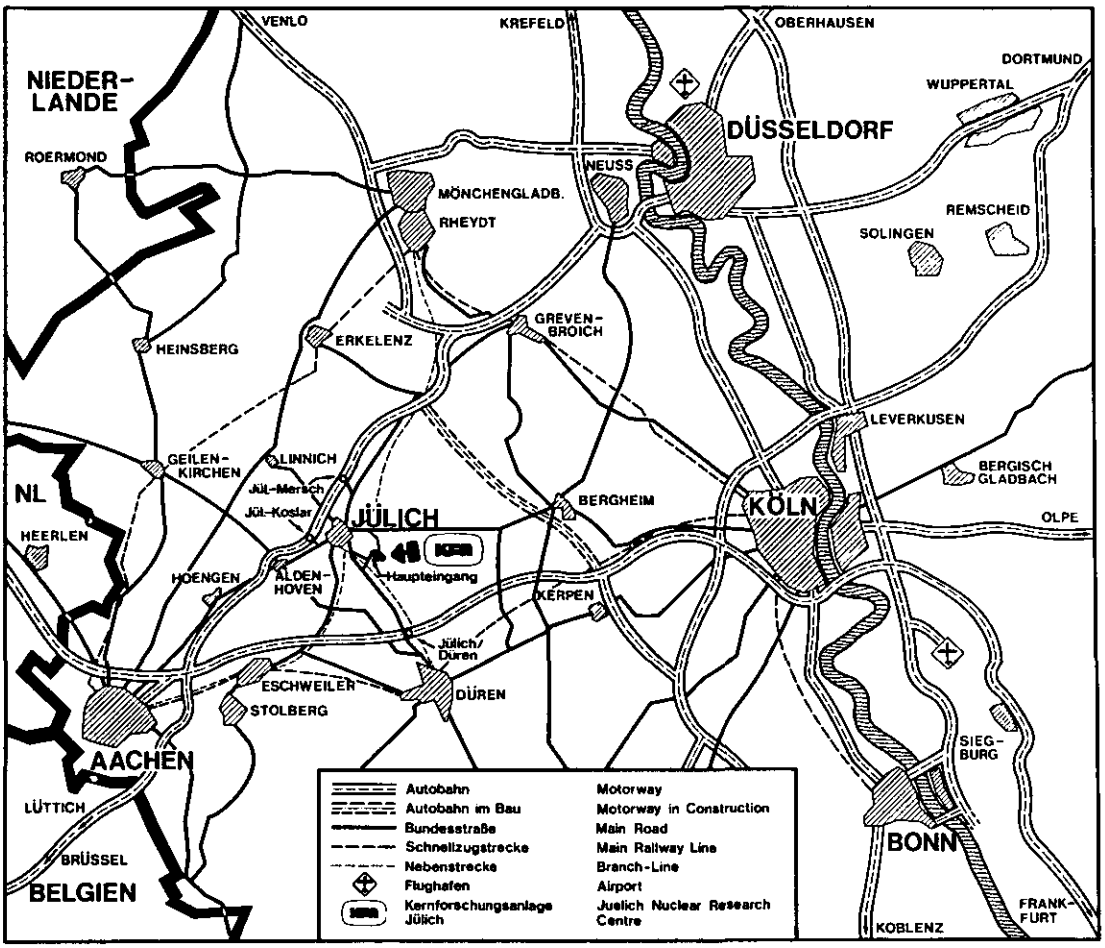

Als Manuskript gedruckt

Spezielle Berichte der Kernforschungsanlage Jülich – Nr. 167

Institut für Reaktorwerkstoffe Jül - Spez - 167

Zu beziehen durch: ZENTRALBIBLIOTHEK der Kernforschungsanlage Jülich GmbH
Postfach 1913 · D-5170 Jülich (Bundesrepublik Deutschland)
Telefon: (0 24 61) 610 · Telex: 8 33 556 kfa d

Graphitic Matrix Materials For Spherical HTR Fuel Elements

Results of Material Development and Irradiation Testing

Catalogue of Pictures and Tables

by

R.-E. Schulze
H. A. Schulze
W. Rind*

* HOBEG Company, Hanau

This report is an extended English language version of the report JÜL - 1752.

GRAPHITIC MATRIX MATERIALS FOR SPHERICAL HTR FUEL ELEMENTS

RESULTS OF MATERIAL DEVELOPMENT AND IRRADIATION TESTING

Catalogue of Pictures and Tables

by

R.-E. Schulze, H.A. Schulze, W. Rind

ABSTRACT

The present report comprises the essential results of material development and irradiation testing of graphitic matrix materials for spherical HTR fuel elements and completes the documentation of the irradiation data for 20 matrix materials (Jül-1702).

The main emphasis is given to the matrices A3-3 (standard matrix) and A3-27 (matrix with synthesized resin), both of which are being used as structural materials for the fuel elements of the AVR and THTR reactors.*) In addition, comparisons are made between 18 A3-variants and the standard matrix A3-3, which show that three of the variants may be considered as a further potential for use. Moreover, the possibilities for HTR fuel elements which are opened up by the introduction of a new technology, warm moulding, are also illustrated.

The results described were obtained within the framework of the HTR project "Hochtemperaturreaktor-Brennstoffkreislauf" (High-Temperature Reactor Fuel Cycle) involving the Gesellschaft für Hochtemperaturreaktor-Technik mbH, Hochtemperaturreaktor-Brennelement GmbH, Hochtemperatur-Reaktorbau GmbH, Kernforschungsanlage Jülich GmbH, NUKEM GmbH and Sigri Elektrographit GmbH/ Ringsdorff-Werke GmbH. The project is sponsored by the "Bundesministerium für Forschung und Technologie" (Federal Ministry for Research and Technology) and by the State of North-Rhine/Westphalia.

---

* for AVR fuel elements: A3-3 and A3-27, for THTR fuel element production: A3-3

CONTENTS
AS WELL AS
LIST OF FIGURES AND TABLES

1. INTRODUCTION

1 INTRODUCTION

A prerequisite for the introduction of high-temperature reactors (HTR) is the provision of adequate test results for spherical fuel elements and their components, coated fuel particles and graphitic matrix.

A comprehensive programme has been carried out for the development and irradiation testing of graphitic matrix materials. The development of materials was performed by NUKEM/HOBEG, Hanau, while irradiations took place in the High Flux Reactor (HFR) Petten, the Netherlands, as part of the joint DRAGON-KFA-EURATOM-RCN/ECN Programme *).

The most significant results of this materials programme are as follows:

1. The development and irradiation testing of graphitic matrix materials have furnished the standard matrix A3-3 which is suitable as a structural material for HTR fuel elements. It is being used for the elements of the AVR**) and the THTR***) reactors and has been proved successfully in AVR reactor operation.
2. The development of variants of the standard matrix with the objectives:
   - enlargement of the raw material base
   - simplification of fabrication
   - improvement of product properties

   and the irradiation testing of 18 of these variants have furnished the matrix with synthesized resin A3-27 which is also suited for use as a structural material for fuel elements. Elements fabricated with this material are already being tested in AVR reactor operation. Three further variants of the standard matrix (A3-6, A3-5 and A5-2) may be considered as a potential for technological use.
3. Influences by raw material, fabrication and irradiation parameters on material properties and their changes under irradiation could be determined. Their knowledge enables a good understanding of the material behaviour.

---

*) Partners involved: OECD-DRAGON Project, Dorchester, Dorset, England; Kernforschungsanlage Jülich GmbH; EURATOM; Stichting Reactor Centrum, Petten, the Netherlands; Stichting Energieonderzoek Centrum, Petten, the Netherlands.

**) Arbeitsgemeinschaft Versuchsreaktor GmbH

***) Thorium High-Temperature Reactor

The present report illustrates essential results of material development and irradiation by means of figures and tables, incorporating the knowledge of materials obtained and irradiation experience acquired.

The main emphasis is given to the matrix materials A3-3 and A3-27, which are being used as structural materials for AVR fuel elements (A3-3 and A3-27) and THTR fuel element production (A3-3).

In addition, comparisons are made between all variants and the standard matrix, using the falling strength*), corrosion rate*) and irradiation behaviour as criteria. Apart from the matrix with synthesized resin A3-27, the materials A3-5, A3-6 and A5-2 have proved to be of technological interest. Compared with the standard matrix they exhibit at least 40 % higher falling strengths and up to 45 % lower corrosion rates along with sufficiently good irradiation behaviour.

---

*) Definition see page 46

2. GRAPHITIC MATRIX FOR SPHERICAL HTR FUEL ELEMENTS

- Application
- Tasks and Requirements

2 GRAPHITIC MATRIX FOR SPHERICAL HTR FUEL ELEMENTS

Application

The graphitic matrix constitutes the structural material for the spherical fuel elements of high-temperature reactors. In the inner fuel zone of the elements the matrix serves as a homogeneous envelopment for the coated fuel particles (Figure 2.1). This fuelled zone has a diameter of 50 mm and is enclosed in a 5 mm thick fuel-free shell. The same matrix material is used for the inner and outer zones of the elements.

Two different matrix materials are currently being applied. The standard matrix A3-3 has been successfully tested for some time already in AVR reactor operation. This material is also used for fuel elements of the THTR reactor. A further material being tested in the AVR reactor is the matrix with synthesized resin A3-27 developed more recently as a variant of the standard matrix.

Tasks and Requirements

The graphitic matrix has to fulfill a number of essential tasks in the fuel element, from which the general material requirements are derived (Figure 2.2).

The matrix in spherical HTR fuel elements

- acts as a moderator for the fission neutrons, with the carbon density being of essential influence;
- performs heat transfer from the coated fuel particles to the surface of the fuel element and must therefore exhibit a good thermal conductivity;
- must guarantee protection against external forces, to which the fuel element is subjected in the core, and must therefore exhibit a high mechanical strength.

Beyond these requirements closely coupled to the tasks of the matrix the following features are of essential significance:

- good resistance to corrosion caused by impurities in the coolant gas,
- high dimensional stability during irradiation with fast neutrons to ensure the pneumatic transfer of fuel elements in the fuelling system.

Application of Graphitic Matrix in Spherical HTR Fuel Elements

Structural material for the fuel elements of the AVR and THTR reactors

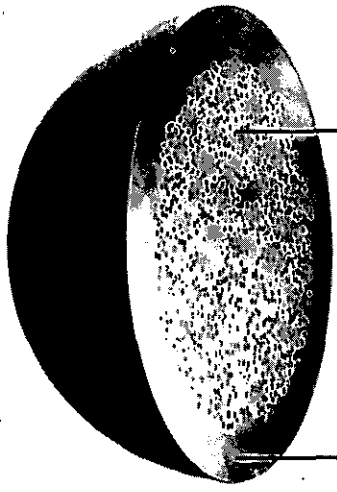

Fuelled zone:

Graphitic matrix used as a homogeneous envelopment of the coated fuel particles

Fuel-free zone:

Graphitic matrix used as a shell of the fuel element

Used in AVR fuel elements:

- Standard matrix A3-3
- Matrix with synthesized resin A3-27

Provided for THTR fuel elements:

- Standard matrix A3-3

2.1

Tasks of Graphitic Matrix in Spherical HTR Fuel Elements

- Moderation of fission neutrons
- Heat transfer from the coated particles to the surface of the fuel element
- Protection of the coated particles against external forces

Demands on the Graphitic Fuel Matrix

- High density
- High thermal conductivity
- High mechanical strength
- Low Young's modulus
- Good corrosion resistance
- Small thermal expansion connected with low anisotropy
- Good dimensional stability under irradiation with fast neutrons
- Nuclear purity

3. PROGRAMME FOR THE DEVELOPMENT AND IRRADIATION TESTING OF GRAPHITIC MATRIX MATERIALS

- Programme Outline
- Material Development
- Fabrication Method
- Irradiation Experiments for Materials Testing
  - Tested Behaviour of Materials
  - Irradiated Matrix Materials

3 PROGRAMME FOR THE DEVELOPMENT AND IRRADIATION TESTING OF GRAPHITIC MATRIX MATERIALS

Programme Outline

Figure 3.1 gives an outline of the programme carried out for the development and irradiation testing of graphitic matrix materials.

Materials Development

The development and optimization of matrix materials by NUKEM/HOBEG was performed in two phases[1] (Figure 3.2). Based on the general requirements to be met by the fuel element, phase I comprised

- the selection of raw materials,
- the introduction of quasi-isostatic cold moulding,
- the development of matrix materials from the raw material components natural graphite, artificial graphite and phenolic resin binder (partly also using soot).

The result of material optimization in this first phase is the standard matrix A3-3 which has the following raw material composition:

64 wt % natural graphite
16 wt % petroleum coke graphite
20 wt % phenolic resin binder.

In phase II of the development, a broad selection of variants of the standard matrix was developed taking into account the specific requirements for the THTR. These variants are subdivided into three groups with different objectives:

1. variants for the enlargement of the raw material base,
2. variants for simplifying fabrication,
3. variants for improving product properties, especially strength.

The following raw material variations were carried out for the first group:

- The natural graphite of the standard matrix was replaced by another natural graphite.

- The artificial graphite of the standard matrix was exchanged for three other different artificial graphites.
- Instead of the highly graphitized artificial graphite of the standard matrix a low-graphitized artificial graphite of the same type of material was used.

The second group is based on the following fabrication variations:

- The final high-temperature treatment of the standard matrix, which formally had been carried out at 1800°C and later on at 1950°C, took place at 1600°C.
- The prefabricated resin binder was replaced by a binder synthesized during the fabrication process, involving also a modification of the binder type.

The third group comprised variations of material composition as well as material components, involving

- a changed ratio of the filler components natural graphite and artificial graphite,
- an increased binder content,
- a modification of the binder type by the addition of a hardener,
- the use of natural graphite of smaller grain size,
- a simultaneous variation of the binder type and grain size of natural graphite

as compared to the standard matrix.

The matrix with synthesized resin A3-27 can be regarded as the result of this second phase of development. It has emerged from the second group of variants and does not only permit simplified fabrication, but also exhibits improved strength and corrosion properties as compared to the standard matrix.

Detailed information about the composition, fabrication, material properties and irradiation behaviour of the two matrix materials A3-3 and A3-27 used for fuel elements is compiled in Chapter 4.

Fabrication Method

Parallel to the development of matrix materials the method for fabricating spherical fuel elements was further developed and standardized by HOBEG.

This method was also used to produce the fuel-free matrix spheres from which the specimens for irradiation experiments were taken. Only the process steps concerning the fuel particles were omitted (Figure 3.3).

The process comprises three main steps:

1. preparation of the raw material mixture,
2. moulding of the fuel-free or fuelled spheres,
3. heat treatment of the spheres.

The pre-mixed filler components natural graphite and petroleum coke graphite are kneaded with the dissolved phenolic resin binder, dried and ground in a hammer mill. This process step is simplified for producing the matrix with synthesized resin: the filler components are warm-mixed with the binder raw materials, phenol and hexamethylenetetramine, while kneading and drying is omitted.

For the fabrication of fuel elements the coated fuel particles are overcoated with resinated powder prior to pressing in a rotating drum, in order to avoid damage due to pressing (typical overcoating thickness e.g. for THTR fuel elements: 100 µm).

The quasi-isostatic cold-moulding operation, in which dies made of silicon rubber are used, consists of two steps:

1. pre-moulding of the fuelled zone of the sphere at a low moulding pressure of 0.3 kN/cm^2,
2. final moulding of the sphere at a moulding pressure of 30 kN/cm^2 after the fuelled zone has been embedded in resinated powder for the sphere shell.

Moulding is followed by mechanical machining of the spheres: lathing to specified size. This is followed by a two-stage heat treatment consisting of carbonization at 800°C and residual degasification at 1800 or 1950°C.

Irradiation Experiments for Material Testing

Within the scope of the overall matrix programme (Figure 3.1), material tests were carried out in the HFR-Petten for testing the matrix materials under

irradiation with fast neutrons. The tests comprised isothermal irradiation experiments with intermediate measurements at regular intervals[2)3)] as well as experiments for the determination of creep data[4)5)] (Figure 3.4).

Material testing in the test series was performed at a maximum of 8 temperature steps in the irradiation temperature range between 400 and 1450°C up to the full THTR operation time dose of 3.5×10^{21} cm^{-2} EDN and partly beyond this. The series consisted of a maximum of 10 part-experiments with measurements of so-called basic data, i.e. specimen dimensions and physical properties, being performed out of pile between the intervals (Figure 3.5).

The irradiation specimens for measuring the basic data were cut out of the inner zone of fuel-free matrix spheres parallel and perpendicular to the equatorial plane (Figure 3.4). The specimens for creep experiments also taken out of the inner zone were of a dumb-bell shape.

Figure 3.6 gives a compilation of the matrix materials irradiated in the isothermal test series as well as information about the respective irradiation temperature range, the accumulated fluence *) and the number of irradiated specimens. This tabulation contains a breakdown of variants of the standard matrix according to their development groups. The materials used for fuel elements are marked in red. The materials representing a potential for technological use are marked in green.

---

*) Most of the specimens have accumulated the full THTR operation time dose ($3.5.10^{21}$ cm^{-2} EDN), only a few reached the minimum or maximum fluences

Programme for Development and Irradiation Testing of Graphitic Matrix Materials for Spherical HTR Fuel Elements

Material development:	NUKEM/HOBEG, Hanau
Irradiations:	Within the framework of the common DRAGON-KFA-EURATOM-RCN/ECN irradiation programme
Partners involved:	OECD-DRAGON Project, Dorchester, England Kernforschungsanlage Jülich GmbH EURATOM, Bruxelles, Belgique Stichting Reactor Centrum, Petten, Nederland (RCN) Stichting Energieonderzoek Centrum, Petten, Nederland (ECN)
Test reactor:	High Flux Reactor (HFR)-Petten, The Netherlands
Measurements:	RCN/ECN-Petten KFA Jülich, Institut für Reaktorwerkstoffe
Data analyses:	KFA Jülich, Institut für Reaktorwerkstoffe
Results:	1. Development of the standard matrix A3-3 2. Irradiation testing of the standard matrix A3-3 3. Development of modifications of the standard matrix 4. Irradiation testing of 18 matrix variants derived from standard matrix
Applications:	Use of 2 proven matrix materials for the spherical fuel elements of the reactors – AVR (standard matrix and matrix with synthesized resin) – THTR (provided: standard matrix)
Potential:	Further materials for technological use

Development of Graphitic Matrix Materials for Spherical HTR Fuel Elements

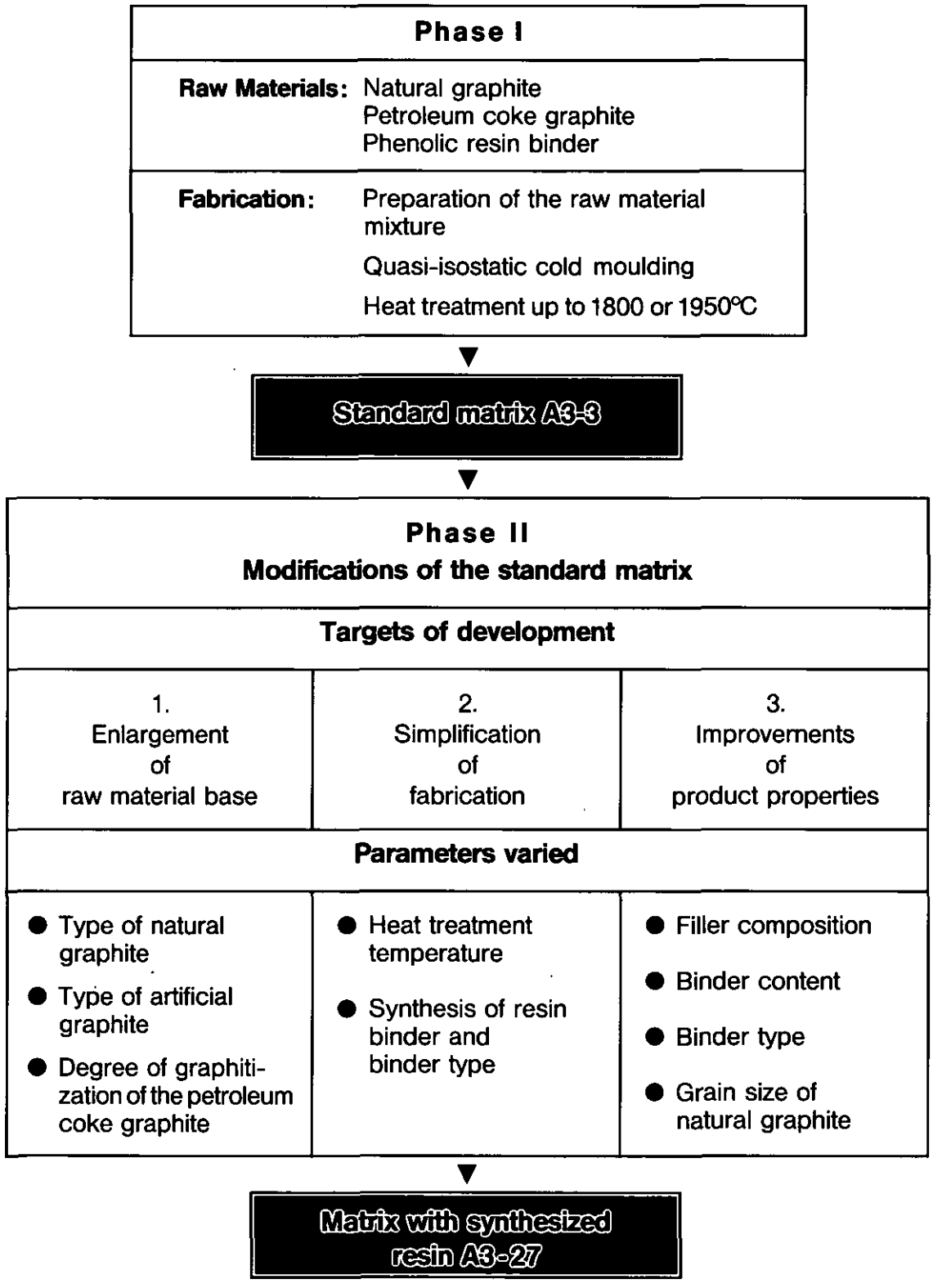

HOBEG Method for Manufacturing Spherical Fuel Elements

(The manufacture of matrix spheres is performed without the steps concerning fuel particles)

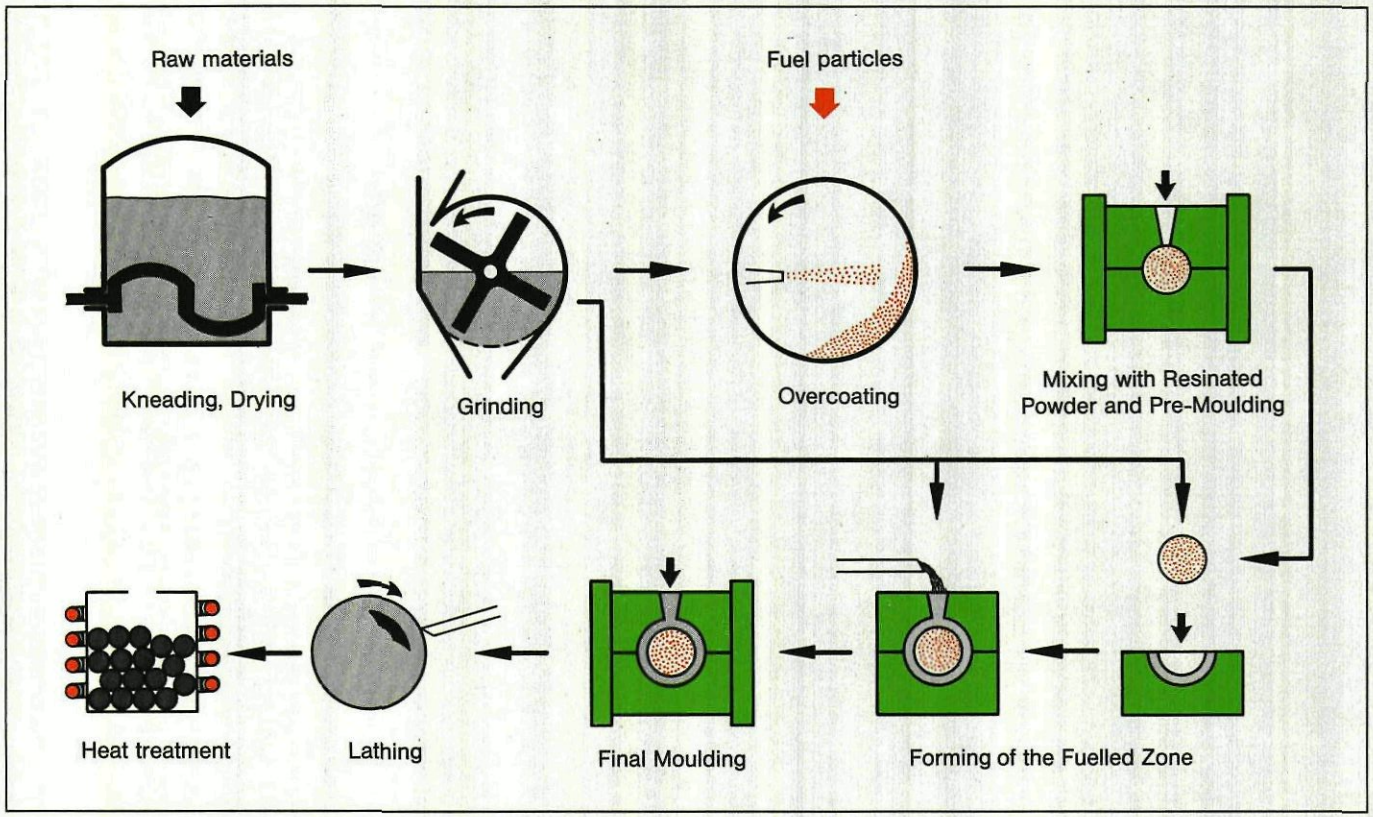

According to M. Hrovat, H. Nickel, K. Koizlik: KFA-Report, Jül - 969 - RW, 1973

3.3

Irradiation Experiments for Testing Graphitic Matrix Materials

- Irradiation experiments
  - Isothermal test series in the HFR Petten
  - Creep experiments in the HFR Petten and in the DRAGON Reactor
- Measurements
  - out of pile between the irradiation intervals
  - Determination of the changes of dimensions and physical properties
  - Determination of creep data
- Irradiation specimens
  - for measurements of basic data

    cut out of fuel-free matrix spheres parallel and perpendicular to the equatorial plane

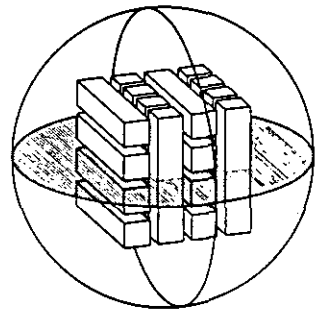

  - for measurements of creep data

    dumb-bell shaped specimens cut out of fuel-free matrix spheres

3.4

Investigated Behaviour of Graphitic Matrix Materials under Fast Neutron Exposure

- Linear dimensional change
- Young's modulus
- Thermal conductivity
- Specific electrical resistance
- Geometrical density
- Coefficient of linear thermal expansion (for A3-3)
- Creep coefficient (for A3-3)

3.5

Graphitic Matrix Materials Irradiated in Isothermal Test Series in the HFR-Petten

Matrix material	Desig-nation	Irradiation temperature (°C)	Accumulated fluence ** (10^{21} cm^{-2} EDN)	Number of specimens
Graphitic standard matrix	A3-3	400 – 1450	2.2 – 8.2	60
Variants for the enlargement of the raw material base	A3-4	450 – 1350	0.8 – 6.3	18
	A3-6	460 – 1400	1.2 – 4.8	12
	A3-10	740 – 1370	1.2 – 4.7	11
	A3-11	600 – 1340	2.1 – 7.9	17
	A3-15	650 – 1400	1.7 – 5.3	15
Variants for simplification of fabrication	A3-7	430 – 1380	1.3 – 4.0	13
	A3-26	450 – 1390	1.4 – 6.6	14
	A3-27/1	430 – 1340	1.2 – 6.6	14
	A3-27/2*	630 – 1420	1.8 – 3.4	10
Variants for improvements of product properties, esp. of strength	A3-5	460 – 1430	1.4 – 4.7	16
	A3-8	600 – 1350	1.3 – 5.5	12
	A3-13	430 – 1350	1.5 – 8.2	11
	A3-16	420 – 1350	0.8 – 10.0	16
	A3-17	680 – 1400	1.7 – 8.4	19
	A3-18	840 – 1350	2.1 – 7.0	4***
	A3-21	900 – 1300	2.7 – 7.4	6
	A5-1	410 – 1320	1.0 – 7.3	11
	A5-2	460 – 1430	1.6 – 9.9	17

* identical with the matrix with synthesized resin, A3-27, being used for AVR fuel elements

** most of the specimens have accumulated the full THTR operation time dose ($3.5 \cdot 10^{21}$ cm^{-2} EDN), only a few reached the minimum or maximum fluences

*** the few results are not reliable enough

4. GRAPHITIC MATRIX MATERIALS USED FOR THE FUEL ELEMENTS OF THE AVR AND THTR REACTORS: STANDARD MATRIX A 3-3 AND MATRIX WITH SYNTHESIZED RESIN A 3-27

- Composition and Fabrication
- Properties of Materials
- Summary of Irradiation Testing
- Irradiation Behaviour of the Standard Matrix A 3-3
  Neutron-Induced Change
  - of Linear Dimension
  - of Young's Modulus
  - of Thermal Conductivity
- Irradiation Behaviour of the Matrix with Synthesized Resin A 3-27
  Neutron-Induced Change
  - of Linear Dimension
  - of Young's Modulus

4 GRAPHITIC MATRIX MATERIALS USED FOR FUEL ELEMENTS OF THE AVR AND THTR REACTORS: STANDARD MATRIX A3-3 AND MATRIX WITH SYNTHESIZED RESIN A3-27

Composition and Fabrication

In Figure 4.1 the most important data concerning raw materials and their composition as well as fabrication are compared for the two matrix materials A3-3 and A3-27 used for the fuel elements of the AVR and THTR reactors. Both materials are based on the same filler components - natural graphite and artificial graphite - and are of similar composition. The essential difference lies in the binder and its processing or its synthesis.

Whereas prefabricated resin binder is processed together with the filler components for fabricating the standard matrix, synthesis of the binder only takes place during the fabrication process for producing the matrix with synthesized resin (cf. Chapter 3). The two phenolic resin binders exhibit differences with regard to the binder type and cross-linking. The phenolic resin binder used for the standard material and produced from phenol and formaldehyde is thermoplastic, and the polymers are cross-linked chiefly two-dimensionally[6]. In contrast, the binder which is synthesized from the raw materials phenol and hexamethylenetetramine for the matrix A3-27 is duroplastic, and the polymers are cross-linked chiefly three-dimensionally[7]. Consequently, the binder cokes forming from the resin binders during heat treatment are of different structure.

The process step of isostatic cold moulding is the same for both matrix materials (cf. Chapter 3). Final high-temperature treatment originally took place at different temperatures. Earlier fuel element reload batches for the AVR reactor, which had been produced with A3-3, as well as matrix spheres for taking out irradiation specimens for material tests were subjected to a heat treatment at 1800°C. For later AVR reload batches and for the THTR production the temperature was increased to 1950°C in order to improve corrosion resistance.

Heat treatment of the fuel elements fabricated with A3-27 was performed exclusively at 1950°C. Only a few fuel elements for high flux tests and some matrix spheres for material testing (pre-production material A3-27/1) were treated at 1800°C.

Material Properties

In Figure 4.2 the material properties of the matrix with synthesized resin A3-27 are compared with those of the standard matrix A3-3. Two sets of data result for the standard matrix, depending on the temperature of 1800°C or 1950°C applied during final heat treatment.

A comparison of these two data sets for the standard matrix shows that an improvement of the corrosion rate is achieved by increasing the temperature during heat treatment from 1800 to 1950°C.

A data comparison between standard matrix and matrix with synthesized resin reveals that the two materials - even when subjected to the same high-temperature treatment - clearly differ in falling strength*) and corrosion rate*), the matrix with synthesized resin exhibiting the better material behaviour.

Material investigations have confirmed that the corrosion resistance of matrix materials is influenced both by the type of binder and by the temperature of heat treatment[8]. This finding helps to explain the different corrosion rates of the materials A3-$3_{1800°}$ and A3-$3_{1950°}$ as well as A3-$3_{1950°}$ and A3-27.

Summary of Irradiation Testing

In order to illustrate the scope of irradiation testing of the fuel element matrix materials A3-3 and A3-27, Figure 4.3 shows

- the ranges of irradiation temperature and the flux of fast neutrons for which changes of the basic data were determined,
- the minimum and maximum fluences accumulated in this connection (cf. footnote p. 12).

*) The characterization tests are described in Chapter 5.

Irradiation Behaviour of the Standard Matrix A3-3

The behaviour of the standard matrix during irradiation with fast neutrons is illustrated in Figures 4.4, 4.5 and 4.6. They show the changes in linear dimension, Young's modulus and thermal conductivity as a function of the fluence. The changes of these basic data are represented as regions limited in each case by the outer isotherms[2)9)].

As can be seen in Figure 4.4, the standard matrix is dimensionally most stable at 900 and 1100°C[*)]. Material shrinkage increases both at lower temperatures (Figure 4.4, left) and higher temperatures (Fig. 4.4, right). Shrinkage of 2 % is reached in connection with the THTR operation time dose at temperatures around 450 and 1250°C[2)]; shrinkage is 2.7 % at the extremely high temperature of 1430°C. As a general result it was found that the standard matrix still is of good dimensional stability and behaves isotropically even under extreme irradiation conditions.

Young's modulus for graphitic matrix materials steeply rises at low fluences and decreases again after having passed a maximum. Rise and decrease depend on temperature. An increase in irradiation temperature reduces the initial rise, lowers the maximum value of relative change and intensifies the decrease[2)10)]. In the case of the standard matrix values between 82 % at 430°C and 33 % at 1430°C were measured for the maximum change of Young's modulus. The fractional change for the THTR operation time dose ranges between +72 % at 430°C and -3 % at 1430°C (Figure 4.5).

The thermal conductivity of the standard matrix decreases monotonously with the fluence in the temperature range between 440 and 1090°C (Figure 4.6). At the lowest measured temperature of 440°C a fluence of 2.5×10^{21} cm^{-2} EDN was accumulated and a change in thermal conductivity of -70 % was determined. In the irradiation temperature range between 1240 and 1360°C thermal conductivity rises again after an initial reduction, and the values reached are up to 5 % higher than prior to irradiation.

---

*) No data are available for 1000°C.

Irradiation Behaviour of the Matrix with Synthesized Resin A3-27

The dimensional change of the matrix with synthesized resin as a function of fluence is shown in Figure 4.7 for irradiation temperatures between 630 and 990°C as well as between 1140 and 1420°C. Data for temperatures below 600°C are not available. It is remarkable that only a very small shrinkage region is observed for temperatures between 630 and 990°C, although the temperature difference amounts to 360°C. The dimensional behaviour of the material is isotropic under irradiation below 1000°C and becomes anisotropic to a limited extent above 1000°C[2)].

Reliable data for Young's modulus are available for the matrix with synthesized resin for the irradiation temperature range between 630 and 1230°C. The maximum value of fractional change is 82 % at 630°C and 40 % at 1230°C.

Comparisons of the matrix materials A3-3 and A3-27 with regard to their dimensional behaviour and Young's modulus under irradiation as well as discussions on the parameters causing an effect are contained in Chapter 9.

Composition and Fabrication of the Matrix Materials Used for the Fuel Elements of the AVR and THTR Reactors*

Material and Fabrication	Standard matrix A3-3	Matrix with synthesized resin A3-27
Composition of raw materials:		
Natural graphite	64 wt %	62.4 wt %
Petroleum coke graphite	16 wt %	15.6 wt %
Resin binder	20 wt %	22.0 wt %
Binder	Phenolic resin prefabricated from phenol and formaldehyde	Synthesized resin 2 synthesized from phenol and hexamethylenetetramine during matrix formation
Moulding method	Quasi-isostatic cold moulding	
High-temperature treatment:		
Fuel elements	1800 or 1950°C	1950°C
Fuel-free matrix spheres	1800°C	1950°C

* for AVR fuel elements: A3-3 and A3-27,
for THTR fuel element production: A3-3

Properties of the Matrix Materials Used for the Fuel Elements of the AVR and THTR Reactors*

Material property			Standard matrix A3-3		Matrix w. synth. resin A3-27
High-temperature treatment			1800°C	1950°C	1950°C
Application			older AVR fuel elements	AVR fuel elements THTR prod.	AVR fuel elements
Young's modulus	(kN · cm^{-2})	∥ **	1020	1000	1070
		⊥ **	991	970	1020
Geometrical density	(g · cm^{-3})		1.70	1.73	1,74
Coeff. of linear therm. expansion 20 - 500°C	(10^{-6} K^{-1})	∥	2.80	2.89	2.43
		⊥	2.92	3.45	2.69
Quotient of Coeff. of therm. expansion	$\alpha_\perp / \alpha_\parallel$		1.07	1.19	1.11
Therm. conductivity at room temperature	(W · cm^{-1} K^{-1})	∥	0.59	0.70	0.69
		⊥	0.63	0.63	0.64
Therm. conductivity at 1000°C	(W · cm^{-1} K^{-1})	∥	0.38	0.41	0.44
		⊥	0.38	0.37	0.39
Spec. electrical resistance	(10^{-3} Ω · cm)	∥	1.56	1.46	1.43
		⊥	1.60	1.48	1.48
Falling strength Fall of a test sphere from a height of 4 m onto A3-3-spheres	(Number of falls till fracture)		521	437	652
Corrosion rate at 1000°C in He of 1 bar with 1 vol. % H_2O (10 h)	(mg · cm^{-2} h^{-1})		1.19	0.97	0.73

* for AVR fuel elements: A3-3 and A3-27, for THTR fuel element production: A3-3

** parallel and perpendicular to the equatorial plane of the matrix sphere

Irradiation Testing of the Matrix Materials Used for the Fuel Elements of the AVR and THTR Reactors*

Tested material behaviour under fast neutron exposure in isothermal experiments	Standard matrix A3-3			Matrix with synthesized resin A3-27		
	Irradiation temperature (°C)	Fast neutron flux ($\frac{10^{14}}{cm^2 s}$ EDN)	Accumulated fluence** ($\frac{10^{21}}{cm^2}$ EDN)	Irradiation temperature (°C)	Fast neutron flux ($\frac{10^{14}}{cm^2 s}$ EDN)	Accumulated fluence** ($\frac{10^{21}}{cm^2}$ EDN)
Linear dimensional change Geometrical density	400 - 1450	0.2 - 2.6	2.2 - 8.2	630 - 1420	0.8 - 2.6	2.0 - 3.4
Young's modulus	400 - 1450	0.2 - 2.6	2.2 - 8.2	630 - 1230	0.8 - 2.2	1.8 - 3.0
Coefficient of linear *thermal expansion*	400 - 1450	0.2 - 2.6	0.8 - 3.4	no measurements		
Thermal conductivity Specific electrical resistance	400 - 1350	0.2 - 2.3	2.2 - 5.2	900 - 1350	1.2 - 2.7	0.8 - 1.7
Creep coefficient	600 - 1350	0.2 - 2.5	0.5 - 5.0	no experiments		

* for AVR fuel elements: A3-3 and A3-27, for THTR fuel element production: A3-3

** most of the specimens have accumulated the full THTR operation time dose ($3.5 \cdot 10^{21}$ cm^{-2} EDN), only a few reached the minimum or maximum fluences

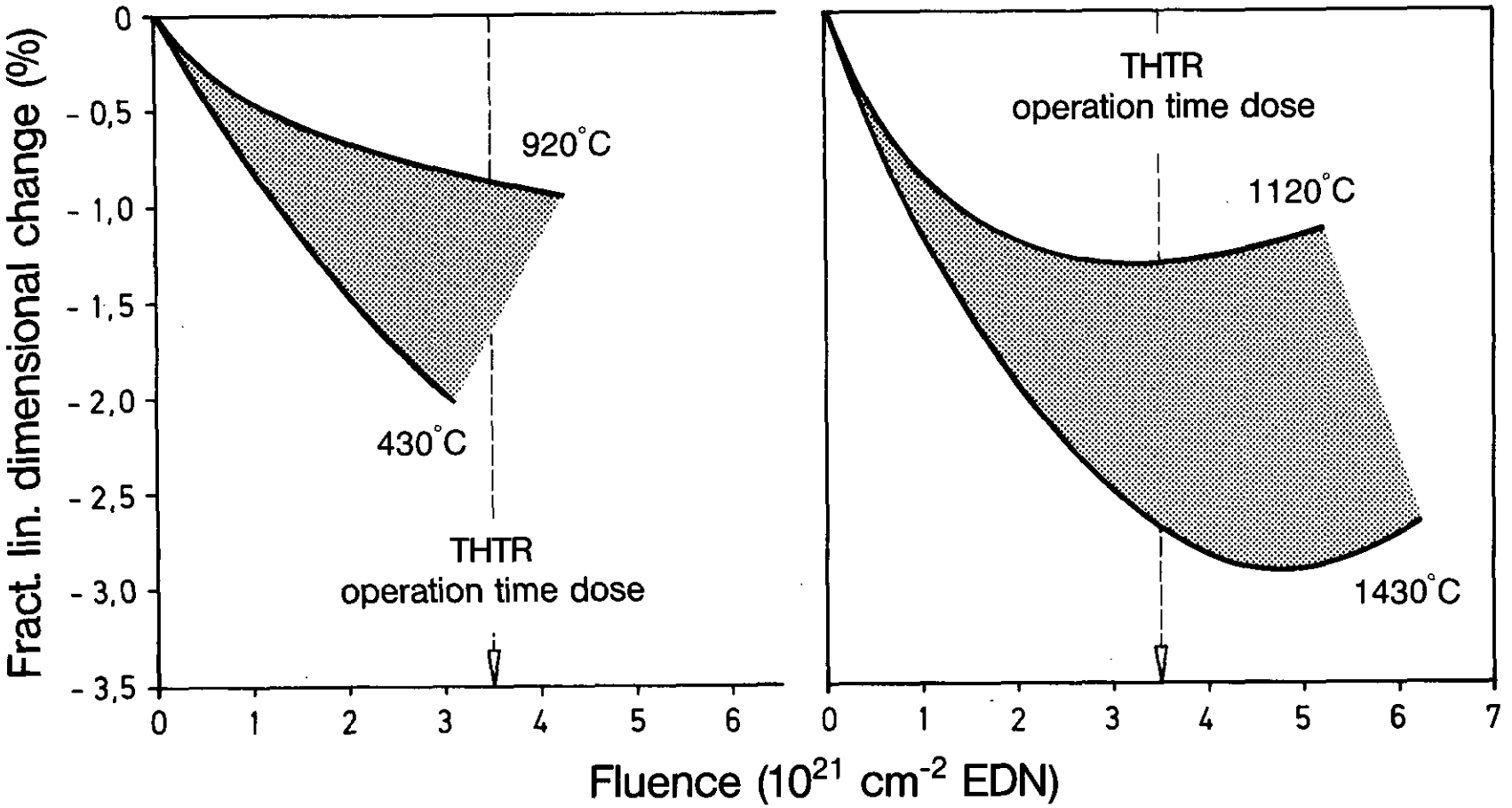

Graphitic Standard Matrix A3-3

Neutron-induced dimensional change for the temperature ranges 430-920 and 1120-1430°C

4.4

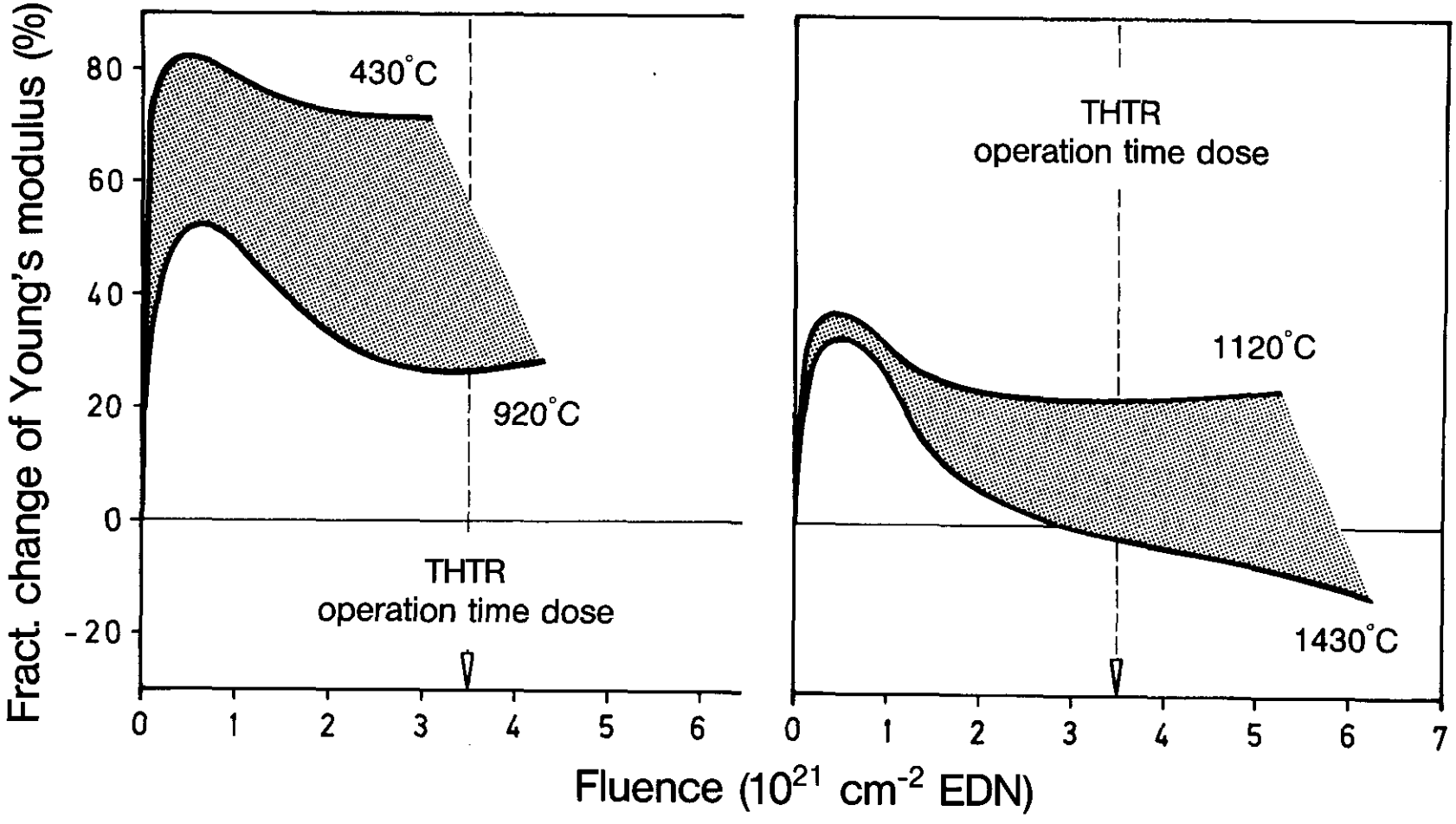

Graphitic Standard Matrix A3-3

Neutron-induced change of Young's modulus for the temperature ranges 430-920 and 1120-1430°C

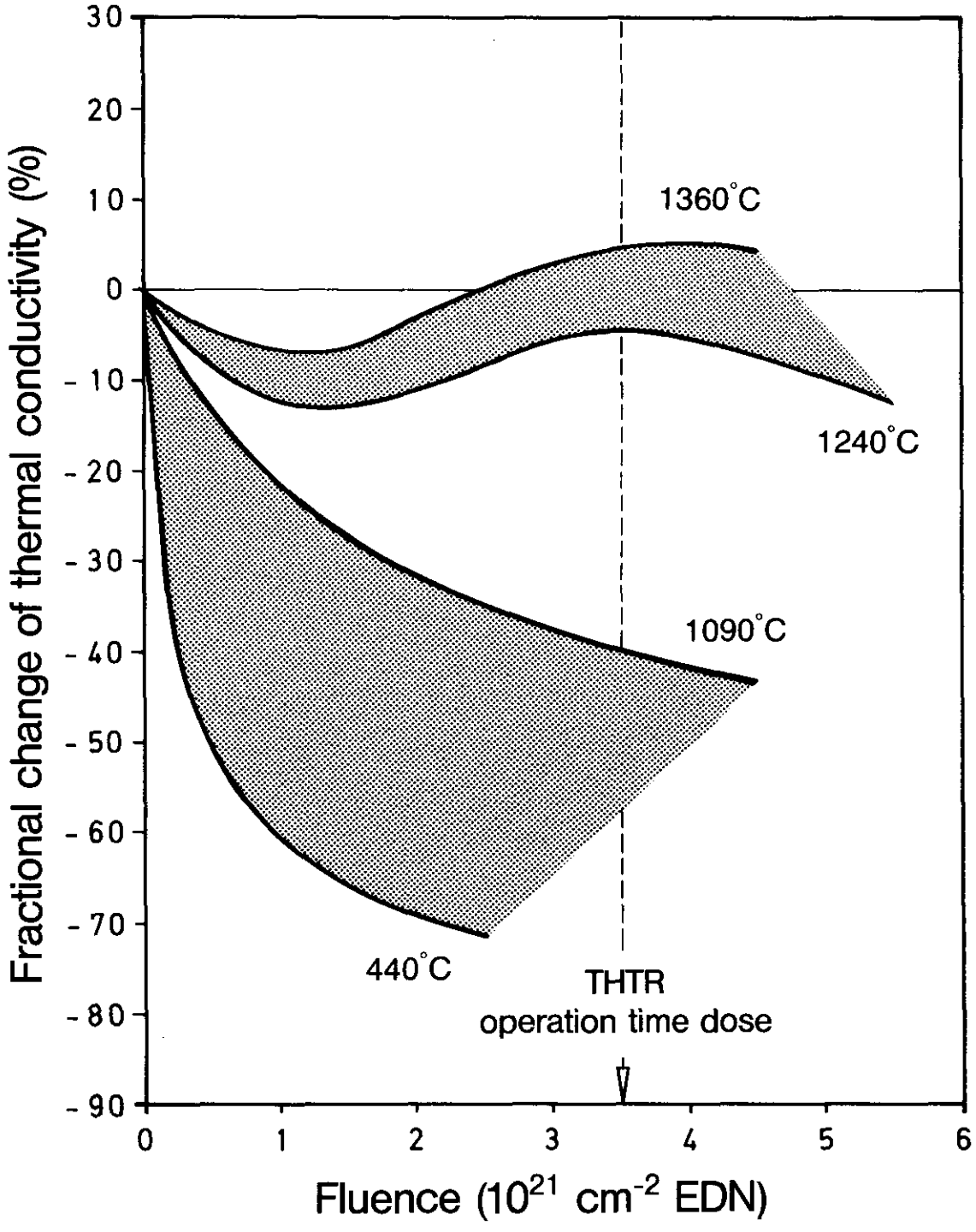

Graphitic Standard Matrix A3-3

Neutron-induced change of thermal conductivity for the temperature ranges 440-1090 and 1120-1430°C, in each case determined at irradiation temperature

(acc. to L. Binkele, High Temp.-High Press., 4, 1972, 401)

4.6

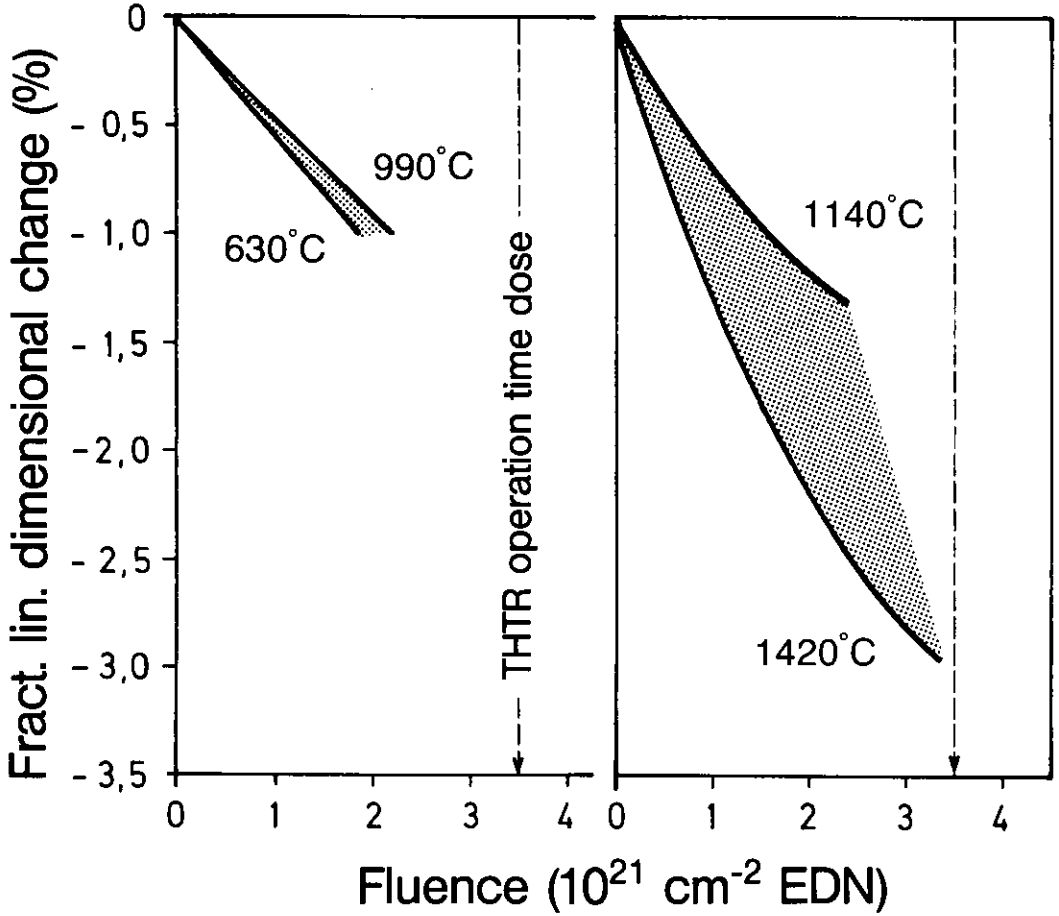

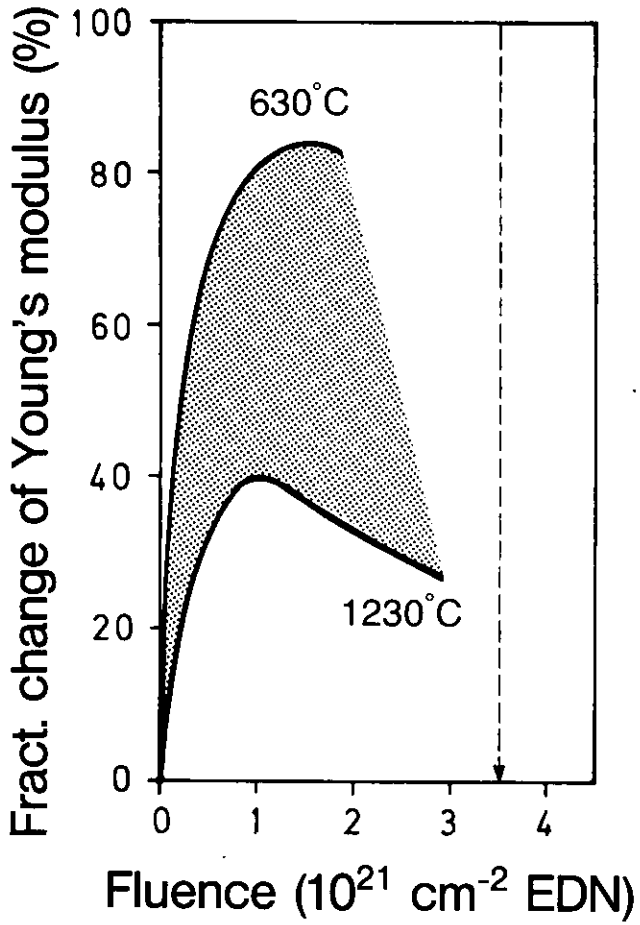

Graphitic Matrix with Synthesized Resin A3-27

Neutron-induced changes of linear dimension and Young's modulus for the temperature range 630-1420 and 630-1230°C, resp.

4.7 **4.8**

5. VARIANTS OF THE STANDARD MATRIX A 3-3 FOR THE ENLARGEMENT OF THE RAW MATERIAL BASE

- Parameter Variations
- Comparison of Raw Material Variants with the Standard Matrix
  Concerning
  - Falling Strength and Corrosion Rate
  - Neutron-Induced Dimensional Behaviour

5 VARIANTS OF THE STANDARD MATRIX A3-3 FOR THE ENLARGEMENT OF THE RAW MATERIAL BASE

Parameter Variations

For an enlargement of the raw material base the filler components, natural graphite and artificial graphite, which are used for fabrication of the standard matrix, were replaced by natural graphite and artificial graphites supplied by other contractors or manufacturers. Since there is little data or information available for the raw materials used, Figure 5.1 specifies the contractors or producers instead of giving information about variations. However, comparisons between the standard matrix and the variants with regard to their irradiation behaviour permit conclusions as to which differences are involved in the raw materials (cf. Chapter 9).

As is shown in Figure 5.1, the raw material variation consisted in a replacement of the natural graphite of the standard matrix by that of a different supplier, while the artificial graphite was exchanged for analogous materials of three other producers. In addition, a type of petroleum coke graphite similar to that of the standard material, but featuring a very low degree of graphitization was used.

Comparison of Raw Material Variants with the Standard Matrix Concerning Falling Strength and Corrosion Rate

Two technologically important material properties were taken as criteria for comparisons between the variants of all development groups and the standard matrix:

- mechanical strength,
- corrosion behaviour.

Determination of the strength and corrosion data was carried out by HOBEG prior to irradiation. The falling and bending strengths were determined for all of the materials, and the tensile and compressive strengths for some of them[1)]. Comparisons were based on the falling strength because of its technological relevance.

The falling strength is defined as the number of falls of a test sphere from a height of 4 m onto a bed of A3-3 spheres until fracture of the test sphere. Between 4 and 80 spheres of the variants and 148 spheres of the standard matrix were subjected to this test within the scope of the determination of data sets forming the basis of the present report[1].

A standard corrosion test was used for characterizing the corrosion behaviour of materials. For this purpose, the corrosion rate was determined in flowing helium at a pressure of 1 bar and with a H_2O content of 1 vol.% after 10 h of annealing at 1000°C.

Table 5.2 shows the falling strengths and corrosion rates of the raw material variants in comparison with those of the standard matrix. All variants exhibit a higher falling strength than the standard material. For two artificial graphite variants, A3-4 and A3-10, there is even an increase of approximately 200 %. The corrosion rates were not determined for all of the materials. Among the data available, only that of the natural graphite variant A3-6 is below that of A3-3. Consequently, the variant A3-6 has proved to be the most favourable raw material variant with regard to both material properties, falling strength and corrosion rate.

Comparison of Raw Material Variants with the Standard Matrix Concerning Neutron-Induced Dimensional Behaviour

Irradiation testing of the raw material variants in the HFR-Petten material tests (cf. Chapter 3) has revealed that, with the exception of the A3-6 variant, the materials clearly differ from the standard matrix A3-3. While the standard material shows an isotropic dimensional behaviour, the variants behave anisotropically under stronger irradiation conditions (Figure 5.3). Moreover, the variant with low-graphitized coke, A3-15, exhibits a turn-around*) which is unusually early and pronounced for matrix materials[2].

Volume shrinkage compared at 1250°C and THTR operation time dose is similar for all materials or even smaller than that of the standard matrix (Figure 5.3). The variant A3-15 has already passed the turn-around under

*) Transition from shrinkage to expansion

these irradiation conditions, and, consequently, exhibits a relatively small shrinkage. Until turn-around its volumetric change corresponds to that of A3-3.

As in the case of material properties, the natural graphite variant A3-6 has therefore proved to be the most favourable raw material variant in respect of neutron-induced dimensional change.

Variations of Parameters for an Enlargement of the Raw Material Base

Parameter	Standard matrix A3-3	Variation	Designation of variant
Type of natural graphite component	Kropfmühl *	Omnium Minier*	A3-6
Type of artificial graphite component	Ringsdorff *	Le Carbone Lorraine* Pechiney * SIGRI *	A3-4 A3-10 A3-11
Degree of graphitization of petroleum coke graphite	high	small	A3-15

* contractor or producer

Matrix Variants for an Enlargement of the Raw Material Base

Comparisons with the Standard Matrix Concerning Falling Strength and Corrosion Rate

Variation		Designation of variant	Falling strength Fall of a test sphere from a height of 4 m onto a bed of A3-3 spheres (Number of falls till fracture)	Corrosion rate 10 h at 1000°C in He of 1 bar with 1 vol. % H_2O (mg · cm^{-2} h^{-1})
			0 500 1000 1500	0 0.5 1.0 1.5
Other type of natural graphite component	Omnium Minier *	A3-6		
	Le Carbone Lorraine *	A3-4		
Other type of artificial graphite component	Pechiney *	A3-10		not determined
	SIGRI *	A3-11		
Smaller degree of graphitization of the petroleum coke graphite comp.		A3-15		not determined
Standard matrix A3-3				

* contractor or producer

Matrix Variants for an Enlargement of the Raw Material Base

Comparisons with the Standard Matrix Concerning Neutron-induced Dimensional Behaviour

Variation		Designation of variant	Dimensional behaviour at THTR operation time dose	Volume shrinkage at 1250°C and THTR operation time dose
Other type of natural graphite component	Omnium Minier *	A3-6	mainly isotropic	slightly smaller than A3-3
Other type of artificial graphite component	Le Carbone Lorraine *	A3-4	anisotropic for T > 700°C	corresponding to A3-3
	Pechiney *	A3-10	anisotropic for T > 1000°C	slightly smaller than A3-3
	SIGRI *	A3-11	anisotropic for T > 900°C	corresponding to A3-3
Smaller degree of graphitization of the petroleum coke graphite comp.		A3-15	anisotropic for T > 1100°C early turn-around	smaller than A3-3 **
Standard matrix A3-3			isotropic	6 vol %

* contractor or producer

** till turn-around corresponding to A3-3 [2)]

6. VARIANTS OF THE STANDARD MATRIX A 3-3 FOR SIMPLIFICATION OF FABRICATION

- Parameter Variations
- Comparison of the Fabrication Variants with the Standard Matrix
  Concerning
  - Falling Strength and Corrosion Rate
  - Neutron-Induced Dimensional Behaviour

6 VARIANTS OF THE STANDARD MATRIX A3-3 FOR SIMPLIFICATION OF FABRICATION

Parameter Variations

In order to simplify and cheapen the fabrication process the final high-temperature treatment of the A3-7 variant was carried out at 1600°C (Figure 6.1) instead of 1800°C (standard matrix).

However, the most important and successful fabrication variation could be achieved by synthesizing the binder during the fabrication process instead of adding prefabricated binder to the filler. This also involves a changed type of binder. The thermoplastic phenolic resin binder made of the raw materials phenol and formaldehyde is replaced by the duroplastic synthesized resin binder formed of phenol and hexamethylenetetramine. The simplification of fabrication consists in the omission of the process steps of kneading and drying as well as the pre-characterization of the resin binder.

Three materials with synthesized resin have been produced (Figure 6.1). The A3-26 variant differs from the other two materials by the type of synthesized resin. Among the variants with the same type of binder, the material A3-27/2 features improvements with regard to material properties as compared to the laboratory scale pre-production material A3-27/1. These were achieved by optimization of the process parameters and by increasing the temperature during final heat treatment.

Comparison of the Fabrication Variant with the Standard Matrix Concerning Falling Strength and Corrosion Rate

Only two of the four fabrication variants exhibit a higher falling strength than the standard matrix, while the other two materials' falling strength is substantially lower (Figure 6.2). Consequently, the materials with synthesized resin, A3-26 and A3-27/1, do not fulfill the requirements to be met in respect of this property. However, their early irradiation testing led to fundamental knowledge permitting an advancement and improvement of materials with synthesized resin. The improved A3-27/2 variant exhibits a falling strength which is by 30 % higher than that of the standardized matrix. Furthermore, its corrosion rate is by 40 % lower and, thus, considerably better than that of the standard material.

For the fabrication variant A3-7 a falling strength was determined which is even above that of the improved material with synthesized resin A3-27/2 (Figure 6.2). On the other hand, the corrosion rate is very high, since the final heat treatment was only carried out at 1600°C. Consequently, the improved matrix with synthesized resin A3-27/2 has proved to be the most favourable fabrication variant with regard to both material properties, falling strength and corrosion rate.

Comparison of the Fabrication Variants with the Standard Matrix Concerning Neutron-Induced Dimensional Behaviour

Testing of the fabrication variants under irradiation revealed that only the variant A3-7 - like the standard matrix - behaves isotropically (Figure 6.3). A different behaviour is observed in each case for specimens of the pre-run materials with synthesized resin, A3-26 and A3-27/1. This may be explained by the relatively large scattering of pre-irradiation data. The improved material with synthesized resin A3-27/2 behaves isotropically below 1000°C and becomes anisotropic above 1000°C. However, the extent of anisotropy remains limited[2].

The volume shrinkage of all materials at 1250°C and THTR operation time dose is similar to that of the standard matrix (Figure 6.3).

These comparisons show that the variant A3-7 corresponds to the standard matrix with regard to its dimensional change and, thus, exhibits the best behaviour of all materials. However, taking into account also the properties of materials, the improved matrix with synthesized resin A3-27/2 turns out to be the most favourable fabrication variant; it is identical with the A3-27 material used for fuel elements (cf. Chapter 4).

Variations of Parameters for Simplification of Fabrication

Parameter	Standard matrix A3-3	Variation	Designation of variant
High-temperature treatment	1800°C	1600°C	A3-7
Binder	Phenolic resin prefabricated characterization necessary	Synthesized resin 1 (thermoplastic) Synthesis during matrix formation	A3-26
		Synthesized resin 2 (duroplastic) Synthesis during matrix formation	A3-27/1 Pre-product. mat. A3-27/2* improved material

* identical with the matrix with synthesized resin A3-27

Matrix Variants for Simplification of Fabrication

Comparisons with the Standard Matrix Concerning Falling Strength and Corrosion Rate

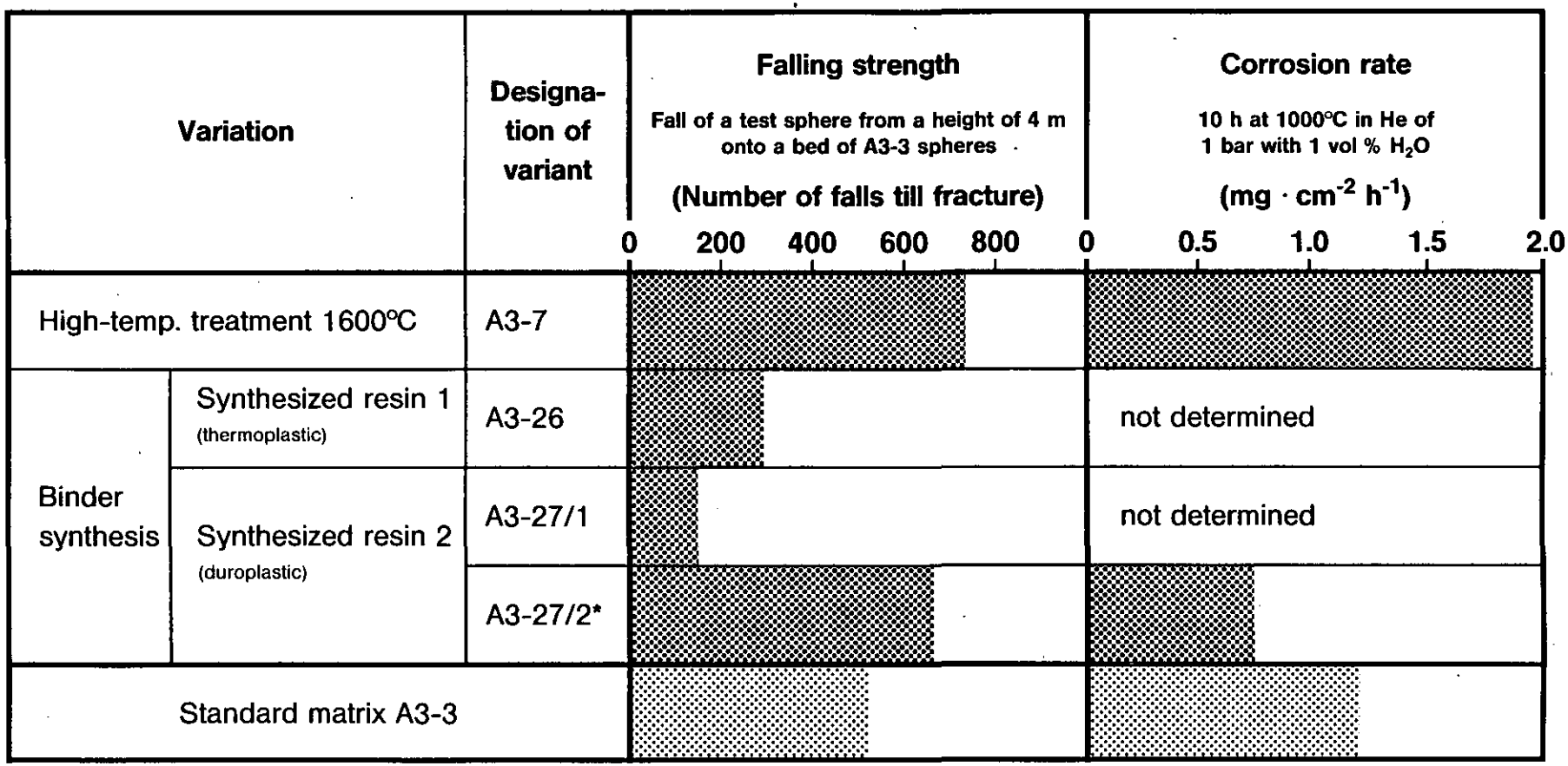

* identical with the matrix with synthesized resin A3-27

Matrix Variants for Simplification of Fabrication

Comparisons with the Standard Matrix Concerning Neutron-induced Dimensional Behaviour

Variation		Designation of variant	Dimensional behaviour at THTR operation time dose	Volume shrinkage at 1250°C and THTR operation time dose
High-temp. treatment 1600°C		A3-7	isotropic	corresponding to A3-3
Binder synthesis	Synthesized resin 1 (thermoplastic)	A3-26	mainly isotropic	slightly smaller than A3-3
	Synthesized resin 2 (duroplastic)	A3-27/1	partly anisotropic for T > 800°C	corresponding to A3-3
		A3-27/2*	anisotropic for T > 1000°C	slightly greater than A3-3
Standard matrix A3-3			isotropic	6 vol %

* identical with the matrix with synthesized resin A3-27

7. VARIANTS OF THE STANDARD MATRIX A 3-3 FOR IMPROVEMENTS OF PRODUCT PROPERTIES, ESPECIALLY OF STRENGTH

- Parameter Variations
- Comparison of the Strength Variants with the Standard Matrix
  Concerning
  - Falling Strength and Corrosion Rate
  - Neutron-Induced Dimensional Behaviour

7 Variants of the Standard Matrix A3-3 for Improvements of Product Properties, Especially of Strength

Parameter Variations

For improvements of product properties, especially for an increase in strength, the material composition as well as the material components were varied (Figure 7.1).

An increase of the natural graphite fraction as compared to that of the standard matrix led to the production of the A3-5 variant which has a filler ratio of natural graphite to artificial graphite of 6 : 1. For the variants A3-8 and A3-13, the binder content was increased as compared to that of the standard matrix. It amounted to 23 and 26 wt %, respectively.

Additions of hardener to the binder lead to changes of the binder type and result in increased binder coke yields[6)11)12)13)]. The variants A3-17, A3-16 and A3-21 were produced with differently high additions of the hardener hexamethylenetetramine. These additions amounted to 5, 10 and 20 wt % related to the binder content.

For the variant A5-1, the natural graphite component used was of the same contractor as that of the standard matrix, but the mean grain size only amounted to 7µm instead of 40 µm.

A simultaneous modification of two parameters proved to be the most successful variation for increasing the strength:
Natural graphite of small grain size (7 µm) as well as a phenolic resin binder with the addition of 10 wt % hardener were used for fabricating the variant A5-2 and caused an increase in strength exceeding by far that of all the other matrix materials.

Comparison of the Strength Variants with the Standard Matrix Concerning Falling Strength and Corrosion Rate

The eight strength variants exhibit highly different, but in all cases clearly higher falling strengths than the standard matrix (Figure 7.2).

Increases amount to at least 20 % and in one extreme case, i.e. for the A5-2 variant, even to more than 900 %. This extreme value suggests that the falling strength to be expected in connection with a bed of spheres made of the test material instead of A3-3 spheres (cf. p. 45) will not be quite as high.

The corrosion rates were only determined for four of these variants. As can be seen from Figure 7.2, all of the values are below that of A3-3. The lowest rates were found in connection with the variants A3-5 and A3-17. They are 40 % below that of the standard material and thus show a considerable improvement of the corrosion behaviour. No corrosion rate has been determined for the A5-2 variant which exhibits the highest falling strength. On account of its material parameters it may however be assumed that the rate is lower than that of the standard matrix (cf. Chapter 8).

A determination of the most favourable variant in respect of both falling strength and corrosion rate is difficult, since the variant featuring a very high falling strength (A5-2) is not identical with any of the variants with low corrosion rate (A3-5 and A3-17). It will only be possible to determine the most favourable variant of this group after comparing the irradiation behaviour of the materials.

Comparison of the Strength Variants with the Standard Matrix Concerning Neutron-Induced Dimensional Behaviour

In contrast to the standard matrix, all strength variants exhibit anisotropic or mainly anisotropic dimensional behaviour at high irradiation temperatures and fluences (Figure 7.3). The extent of anisotropy is different for the materials[2]. Strongly anisotropic behaviour was only observed for the A3-16 variant whose material data were also clearly anisotropic prior to irradiation[11]. Anisotropy for the variants A3-5 and A5-2 remains within reasonable limits[2].

For the majority of strength variants, volume shrinkage at 1250°C and THTR operation time dose is greater than that of the standard matrix (Figure 7.3). Only the variant A5-2 shows a corresponding shrinkage, while variant A3-5 even remains below that of A3-3.

Consequently, the materials A3-5 and A5-2 prove to be the most favourable strength variants with regard to neutron-induced dimensional change and material properties. Two favourable variants therefore result from this group, of which

- the material A3-5 exhibits a particularly good corrosion behaviour and
- the material A5-2 has a very high falling strength.

Variations of Parameters for Improvements of Product Properties, especially of the Strength

Parameter		Standard matrix	Variation	Designation of variant
Ratio of natural graphite to artificial graphite		4 : 1	6 : 1	A3-5
Binder content		20 wt %	23 wt % 26 wt %	A3-8 A3-13
Hardener addition *		without hardener	5 wt % 10 wt % 20 wt %	A3-17 A3-16 A3-21
Mean grain size of the natural graphite component	without hardener	40 µm	7 µm	A5-1
	10 wt % * hardener	–	40 µm 7 µm	A3-16 A5-2

* related to the binder content

Matrix Variants for Improvements of Product Properties, especially of the Strength

Comparisons with the Standard Matrix Concerning Falling Strength and Corrosion Rate

Variation		Designation of variant	Falling strength Fall of a test sphere from a height of 4 m onto a bed of A3-3 spheres (Number of falls till fracture) 0 1000 2000	Corrosion rate 10 h at 1000°C in He of 1 bar with 1 vol % H_2O (mg · cm^{-2} h^{-1}) 0 0.5 1.0 1.5
Ratio of natural graphite to artificial graphite = 6 : 1		A3-5		
Binder content	23 wt %	A3-8		not determined
	26 wt %	A3-13		
Addition of hardener to the binder (related to the binder content of the standard matrix)	5 wt %	A3-17		
	10 wt %	A3-16		
	20 wt %	A3-21		not determined
Mean grain size of the natural graphite component 7 µm	without hardener	A5-1		not determined
	10 wt % hardener	A5-2	> 5000	not determined
Standard matrix A3-3				

7.2

Matrix Variants for Improvements of Product Properties, especially of the Strength

Comparisons with the Standard Matrix Concerning Neutron-induced Dimensional Behaviour

Variation		Designation of variant	Dimensional behaviour at THTR operation time dose	Volume shrinkage at 1250°C and THTR operation time dose
Ratio of natural graphite to artificial graphite = 6 : 1		A3-5	mainly anisotropic for T > 800°C	smaller than A3-3
Binder content	23 wt %	A3-8	mainly anisotropic for T > 1000°C	greater than A3-3
	26 wt %	A3-13	anisotropic for T > 1000°C	greater than A3-3
Addition of hardener to the binder (related to the binder content of the standard matrix)	5 wt %	A3-17	anisotropic for T > 900°C	greater than A3-3
	10 wt %	A3-16	strongly anisotropic for T > 900°C	greater than A3-3
	20 wt %	A3-21	anisotropic for T > 900°C	greater than A3-3
Mean grain size of the natural graphite component 7 µm	without hardener	A5-1	anisotropic for T > 1000°C	greater than A3-3
	10 wt % hardener	A5-2	anisotropic for T > 700°C	corresponding to A3-3
Standard matrix A3-3			isotropic	6 vol %

8. MOST FAVOURABLE VARIANTS FOR THE ENLARGEMENT OF THE RAW MATERIAL BASE, SIMPLIFYING FABRICATION AND IMPROVING STRENGTH

- Compilation of the Most Favourable Variants
- Influences Causing an Improvement of the Falling Strength and Corrosion Rate

8 Most Favourable Raw Material, Fabrication and Strength Variants

Compilation of Most Favourable Variants

In Figure 8.1 those materials are compiled which have emerged as most favourable variants from the three development groups with the objectives

- enlargement of the raw material base,
- simplification of fabrication,
- improvement of product properties

(Chapters 5 to 7).

These variants exhibit at least 30 % higher falling strengths and up to 45 % lower corrosion rates than the standard matrix. Under strong irradiation conditions, the volume shrinkage of all materials is similar to that of A3-3; the dimensional behaviour becomes anisotropic in the case of three of the variants, however, to a limited extent[2].

Of the four most favourable materials, the variant A3-27/2 (identical with the matrix with synthesized resin A3-27) is already being used as structural material for AVR fuel elements (cf. Chapter 4). Moreover, the raw material variant A3-6 as well as the strength variants A3-5 and A5-2 constitute a potential of technologically interesting matrix materials exhibiting improved strength and corrosion properties as well as a sufficiently good dimensional behaviour under irradiation.

Raw materials availability and low cost would be added as further criteria in the event of technological application.

Influences Improving the Falling Strength and Corrosion Rate

The material comparisons made in Chapters 5 to 7 not only show which variants may be regarded as a potential for technological use, but they furthermore indicate which influences have led to their favourable strength and corrosion properties. This shows the paths opening up in the event of increasing requirements.

Data analyses have revealed that the interaction between filler and binder plays a significant role for the strength of graphitic matrix[11]. Under equal conditions of manufacture, this is again influenced by

- the type of natural graphite and artificial graphite filler components,
- the filler grain size,
- the type of binder,
- the ratio of binder coke content to filler content.

In conjunction with this filler-binder coke bonds are formed with different macroscopic properties[10)11)].

The highest falling strength of the matrix was achieved by simultaneous variation of two material parameters (cf. Figure 8.1, variant A5-2):

- reduction of the grain size of the natural graphite component from 40 to 7 µm,
- addition of 10 wt % hardener to the binder.

Three of the above-mentioned parameters are effective in this case:

- the filler grain size,
- the type of binder,
- the ratio of binder coke content to filler content.

By reducing the grain size of natural graphite the overall surface of the grains is enlarged and the interaction between filler and binder is thus intensified.

The addition of a hardener to the binder leads to an increase of the binder coke content, on the one hand, and to a changed type of binder, on the other hand (cf. Chapter 7).

By increasing the binder coke content, the ratio of binder coke content to filler content is adapted to the enlarged grain surface and a largely isotropic distribution of filler grains is thus achieved.

Due to a higher binder cross-linking, the change in the binder type leads to the formation of a binder coke with modified structure, resulting in a buildup of local stresses in the matrix[6)11)12)13)].

The stresses can be substantially reduced, however, if there is a strong interaction between filler and binder as in the present case. This is demonstrated, in particular, by the irradiation behaviour which hardly reveals any effects of increased stresses in the material[11].

This balanced combination of two different material variations thus implies a series of mutual effects and leads to a matrix material which exhibits extremely good strength properties, in particular a very high falling strength and largely isotropic material properties.

It may be seen from the manifold variations of production and material parameters that an improvement in the corrosion behaviour of the matrix can be ultimately attributed to

- a reduction of elements promoting corrosion,
- a decrease of binder coke reactivity.

Both effects become manifest in the case of the matrix with synthesized resin A3-27 and lead to a 40 % lower corrosion rate as compared to the standard material (Figure 8.1).

The improvement achieved is attributable to the following effects:

Owing to the binder synthesis during the process of matrix fabrication, impurities promoting corrosion in a catalytic manner are introduced into the matrix to a smaller extent than in connection with the use of prefabricated resin binder[15].

The increase in temperature from 1800 to 1950°C during heat treatment causes an intensified reduction of existing elements promoting corrosion. On the other hand, it leads to an increase in the degree of graphitization of the binder coke component, reducing its reactivity and thus increasing the corrosion resistance of the matrix[8)16].

The change of the binder type results in a modified binder coke structure, due to a stronger cross-linking of the binder, reducing the corrosion rate of the matrix[8].

The favourable influence which can be exerted on the corrosion rate of the matrix by increasing the temperature during final heat treatment was also utilized in the fabrication of fuel elements for the THTR (cf. Chapter 4). After high-temperature annealing at 1950°C, the standard matrix A3-3 used as structural material showed a 20 % lower corrosion rate than after annealing at 1800°C.

Most Favourable Variants for an Enlargement of the Raw Material Base, Simplification of Fabrication and Improvement of Strength Concerning Falling Strength and Corrosion Rate as well as the Neutron-induced Dimensional Behaviour

Variant	Variation	Falling strength related to A3-3	Corrosion rate related to A3-3	Dimensional behaviour at THTR operation time dose	Volume shrinkage at 1250°C and THTR operation time dose
A3-6 (enlargement of raw material base)	Other type of natural graphite component	150 %	55 %	mainly isotropic	slightly smaller than A3-3
A3-27/2* (simplification of fabrication)	Binder synthesis	130 %	60 %	anisotropic ** for T > 1000°C	slightly greater than A3-3
A3-5 (improvement of strength)	Elevated content of natural graphite	140 %	60 %	mainly anisotropic ** for T > 800°C	smaller than A3-3
A5-2 (improvement of strength)	Smaller grain size of natural graphite and addition of hardener	> 1000 %	not determined	anisotropic ** for T > 700°C	corresponding to A3-3

* identical with the matrix with synthesized resin A3-27

** anisotropic behaviour to a limited extent [2)]

9. COMPARISON OF THE IRRADIATION BEHAVIOUR OF THE MOST FAVOURABLE VARIANTS WITH THAT OF THE STANDARD MATRIX CONCERNING LINEAR DIMENSION AND YOUNG'S MODULUS

- Most Favourable Raw Material Variant A 3-6
  - Linear Dimension
  - Young's Modulus
- Most Favourable Fabrication Variant A 3-27
  - Linear Dimension
  - Young's Modulus
- Favourable Strength Variant A 3-5
  - Linear Dimension
  - Young's Modulus
- Favourable Strength Variant A 5-2
  - Linear Dimension
  - Young's Modulus

9 Comparison of the Irradiation Behaviour of the Most Favourable Variants with that of the Standard Matrix Concerning Linear Dimension and Young's Modulus

In Chapters 5 to 8 the isotropy and anisotropy of the dimensional behaviour and the volumetric change were already discussed as evaluation criteria for the irradiation behaviour of the variants of the standard matrix under strong irradiation conditions.

The present chapter illustrates the behaviour under irradiation of the four technologically interesting variants A3-6, A3-27, A3-5 and A5-2. Figures 9.1 to 9.8 show the materials' changes in linear dimension and Young's modulus, dependent on fluence, in comparison with those of the standard matrix. The test target of irradiations, i.e. the full THTR operation time dose of 3.5 x 10^{21} cm^{-2} EDN, has been marked in each specific case. The influence of both material and fabrication variations is being discussed for a better understanding of the irradiation behaviour.

Most Favourable Raw Material Variant A3-6

The most favourable raw material variant A3-6, for which a natural graphite other than that of the standard matrix was used (cf. Chapter 5), features a smaller dimensional change than the standard material at all comparable irradiation temperatures (Figure 9.1) while Young's modulus shows a slightly stronger change (Figure 9.2).

There is hardly any information available about the natural graphite used as raw material for this variant. However, the irradiation behaviour of the matrix A3-6 indicates that there must be differences as compared to the natural graphite of the standard matrix despite the same geographical origin. This is confirmed primarily by the behaviour of Young's modulus under irradiation whose greater change in the range of low fluences suggests a stronger influence of the neutron-induced pinning effect [17]. Since this effect, which is due to the pinning of mobile dislocations caused by irradiation-induced point defect clusters, has an influence in the crystalline and well-ordered regions of the material and since no other material

parameter except natural graphite was changed, there must be differences in the type of natural graphite filler as regards its crystalline nature.

The filler-binder arrangement and thus the texture and structure of the material can be changed due to differences in the filler type. Such a cause is indicated by the higher initial density of the variant as compared to that of the standard matrix, which may explain the smaller neutron-induced shrinkage of the material. Of importance in this connection is also the lower open porosity which, besides less corrosion-promoting impurities, constitutes a prerequisite for the remarkably low corrosion rate of the variant (cf. Figure 8.1).

Most Favourable Fabrication Variant A3-27

The matrix with synthesized resin A3-27, which has proved to be the most favourable fabrication variant and is being used in AVR fuel elements, was already described in detail in Chapters 4 and 6. Since it differs from the standard material by

- the type of binder,
- the binder coke content,
- the temperature during final heat treatment,

influences caused by all three parameters are to be considered when comparing the irradiation behaviour.

As is shown in Figure 9.3, the dimensional change of the matrix with synthesized resin is clearly smaller than that of the standard matrix at the lowest reference temperature (630°C); however, it shrinks more than A3-3 at temperatures above 1000°C and the dimensional behaviour becomes anisotropic, although this anisotropy remains within a limited extent[2)]. The change of Young's modulus for this variant is greater than that of the standard matrix at all temperatures (Figure 9.4).

The three parameters mentioned above, by which the matrix with synthesized resin differs from the standard matrix, have different and, in part, counteracting effects on the dimensional behaviour of the material:

The increased temperature during final heat treatment is of greatest significance . It results in a higher initial density of the matrix and better preordering of its binder coke component. Therefore, under irradiation, a lower densification of the matrix and a lower irradiation-induced graphitization of the binder coke occur. Both effects cause a higher dimensional stability of the material[8)18)].

A counteracting effect of intensified neutron-induced shrinkage results from the different type of binder and the higher binder coke content. Due to the higher cross-linking of the binder, an increased stress-induced graphitization of the binder coke occurs during irradiation and as a result of the higher binder coke content more poorly graphitized material fractions are subjected to the increased irradiation-induced graphitization[11)18)].

The greater change in Young's modulus for the variant A3-27 as compared to that of the standard material cannot be explained satisfactorily by means of the parameters causing effects on dimensional change. Irradiation experience has shown, however, that the behaviour of Young's modulus under irradiation is influenced even by slight material variations[10)], so that other influences which have not been discussed here may play a role in this connection.

Favourable Strength Variant A3-5

The variant A3-5 produced with a higher fraction of natural graphite than the standard matrix also exhibits a considerably better corrosion behaviour in addition to higher strength (cf. Chapters 7 and 8).

Figure 9.5 shows that this variant has a greater dimensional stability than the standard material under irradiation. At temperatures above 800°C the dimensional behaviour becomes anisotropic to a limited extent[2)]. The neutron-induced change of Young's modulus is only slightly greater for this variant as compared to that of the standard matrix (Figure 9.6).

Influential parameters resulting for the variant A3-5 from a comparison of the irradiation behaviour of the two materials are

- the initial density or initial porosity,
- the natural graphite fraction of the filler[10)].

At low irradiation temperatures, A3-5 undergoes a lower densification than the standard matrix on account of its higher initial density and therefore exhibits greater dimensional stability. Additional influences are only effective at higher temperatures due to the changed ratio of the filler components:

Due to the increased highly crystalline fraction of natural graphite, which replaces a corresponding fraction of the less well graphitized artificial graphite, fewer artificial graphite fractions are subjected to neutron-induced graphitization during irradiation. Consequently, the associated shrinkage of the matrix A3-5 is smaller than that of the standard material. An adverse influence of the higher natural graphite fraction is the increasingly anisotropic dimensional behaviour, although the material properties are largely isotropic prior to irradiation.

The behaviour of Young's modulus for the variant A3-5 also points to effects which are due to the influential parameters mentioned above:

The slightly higher change of Young's modulus in the range of low fluences as compared to that of the standard matrix is due to the higher fraction of highly crystalline natural graphite for which a stronger neutron-induced pinning effect can be assumed[17] (cf. p. 79). In the range of higher fluences and temperatures there is a superposition of effects which, on the one hand, are attributable to irradiation-induced graphitization of the artificial graphite component and, on the other hand, to the change in porosity of the matrix[10].

Favourable Strength Variant A5-2

This variant, which differs from all the other matrix materials by its very high falling strength, was fabricated using very fine-grained natural graphite and adding a hardener to the binder (cf. Chapters 7 and 8).

As is shown in Figure 9.7, the neutron-induced dimensional change of the variant A5-2 is predominantly larger than that of the standard material, but shrinkage values around 2 % are only reached in connection with the full THTR operation time dose at the temperatures relevant for the THTR fuel element. Anisotropic behaviour is observed above 800°C, but the extent of anisotropy remains limited[2].

Clear differences may be observed between the neutron-induced changes of Young's moduli for both materials (Figure 9.8). In comparison with the standard matrix, the variant shows a less steep initial rise of Young's modulus, a lower maximum value of fractional change as well as a smaller subsequent decrease. This favourable behaviour under irradiation is opposed to the undesired high value for Young's modulus prior to irradiation[2]. Nevertheless, the same parameters of influence are effective:
The relatively high modulus of elasticity of the variant prior to irradiation as compared to that of the standard matrix is due to the low porosity of the material, on the one hand, which is connected with the reduced grain size of natural graphite; on the other hand, it is a consequence of the higher fraction of the poorly graphitized binder coke component.

Under irradiation the smaller filler grain and the higher binder coke fraction contribute to reducing the initial rise of Young's modulus and to lowering the maximum value. This is caused by the neutron-induced pinning effect[17] which is less or hardly effective in the filler regions with very small grain and in the poorly ordered binder coke regions and, thus, leading to a smaller change in Young's modulus. Further influences due to the neutron-induced change in porosity of the material and to irradiation-induced graphitization of the binder coke component affect the behaviour of Young's modulus only under stronger irradiation conditions[10].

Influential parameters are also perceivable for the neutron-induced dimensional change of the variant, and they all contribute to material shrinkage: Due to the higher binder coke content and to the change in the type of binder coke caused by the addition of a hardener, irradiation-induced graphitization of the binder coke component is intensified, resulting in an increased shrinkage of the matrix[11].

An additional shrinkage effect may be attributed to a process of neutron-induced re-ordering in the very small grains of natural graphite, since the structure has been changed and the crystallite size reduced by the grinding process[6].

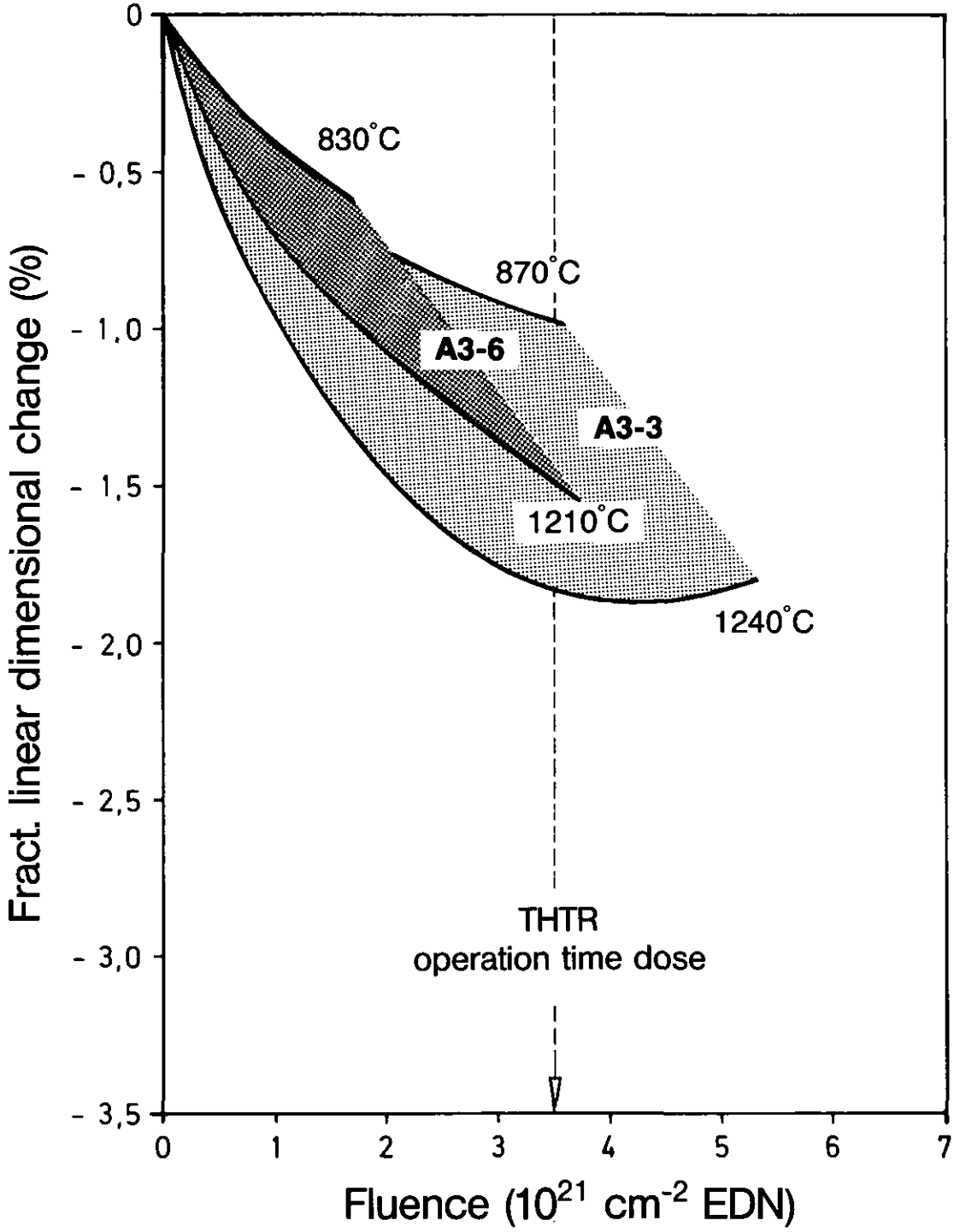

Most Favourable Variant
for an Enlargement of the Raw Material Base A3-6

Comparison of the neutron-induced dimensional change with that of the standard matrix A3-3

9.1

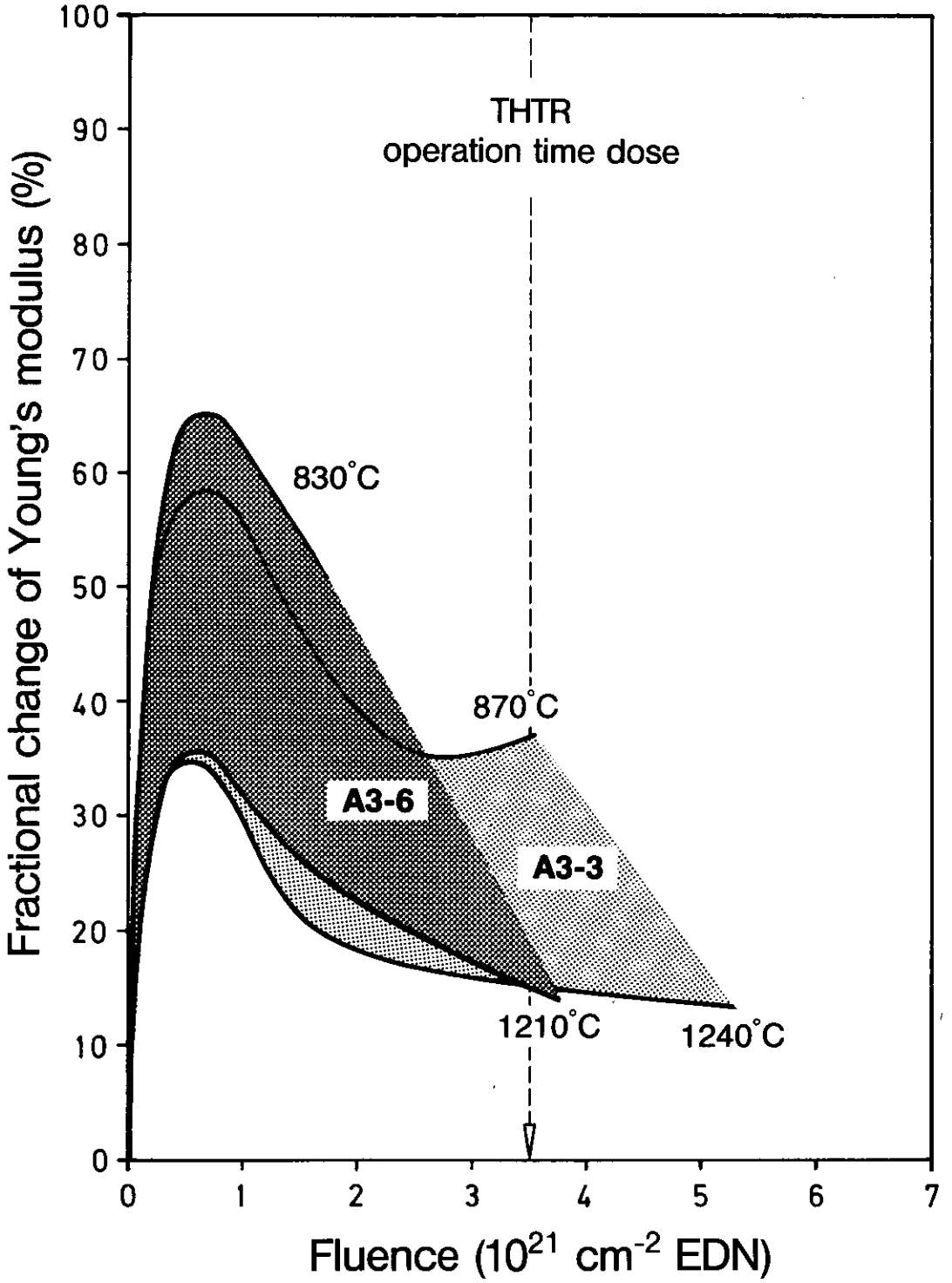

Most Favourable Variant
for an Enlargement of the Raw Material Base A3-6

Comparison of the neutron-induced change of Young's modulus with that of the standard matrix A3-3

9.2

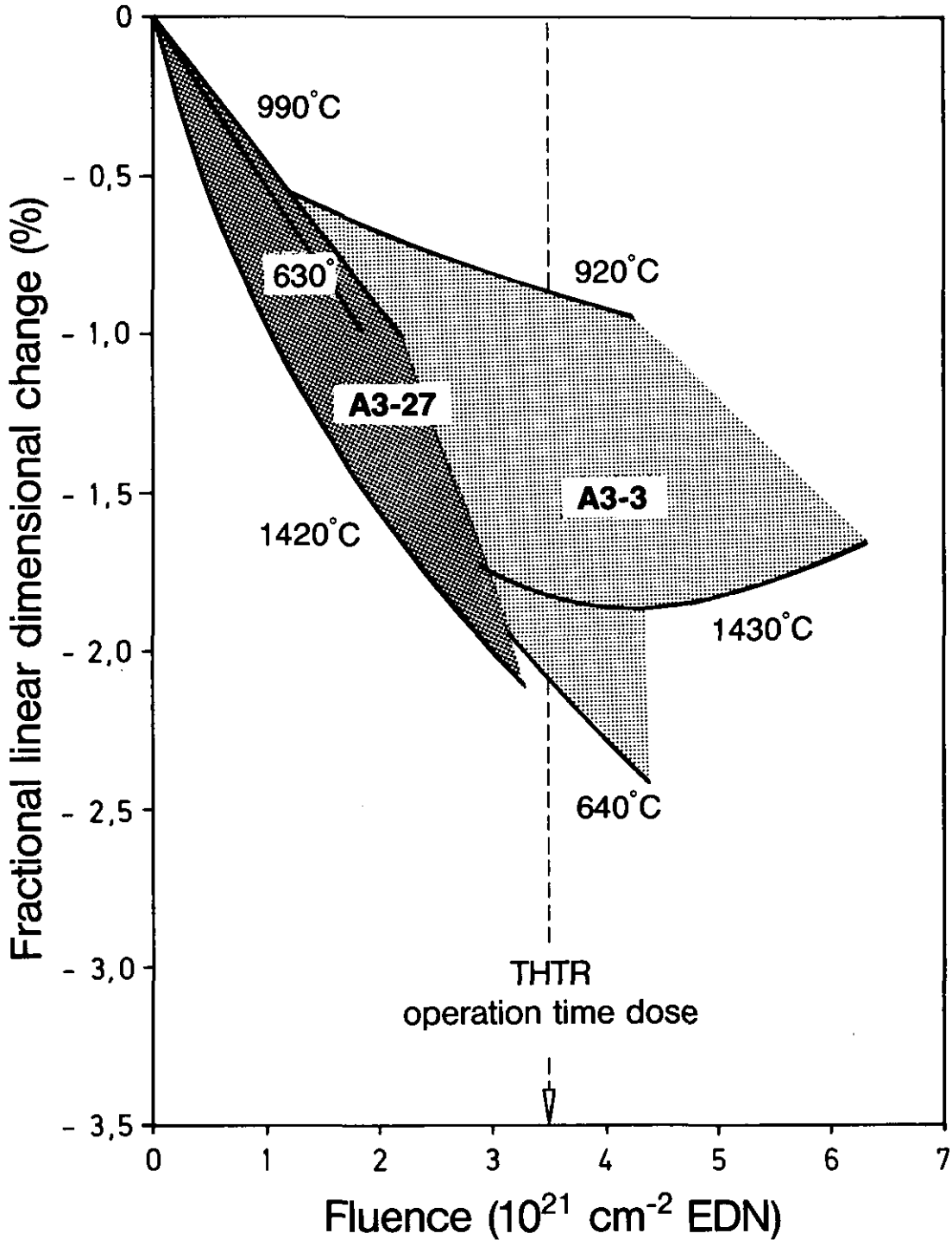

Most Favourable Variant for Simplification of Fabrication A3-27

Comparison of the neutron-induced dimensional change with that of the standard matrix A3-3

9.3

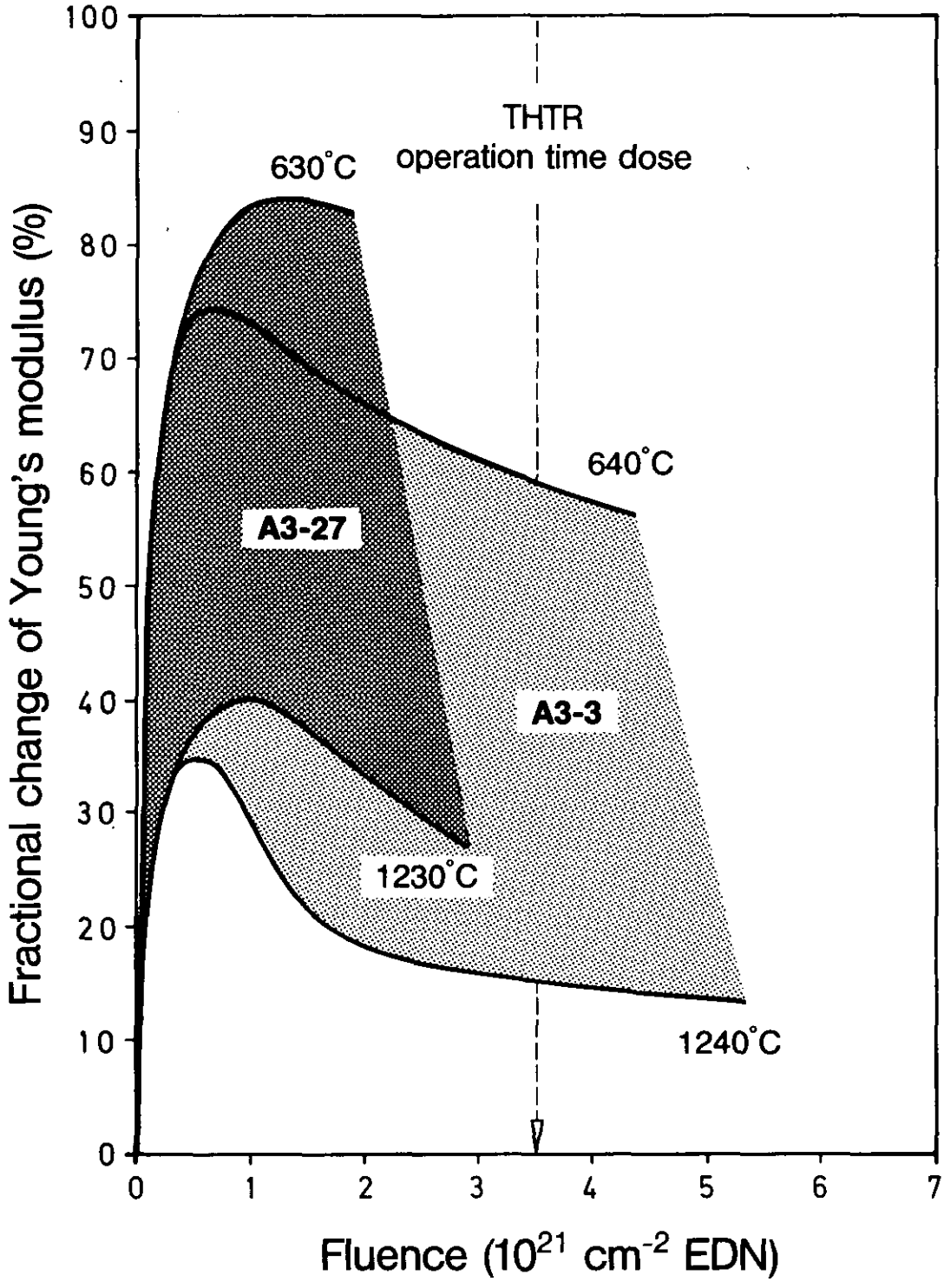

Most Favourable Variant
for Simplification of Fabrication A3-27

Comparison of the neutron-induced change of Young's modulus with that of the standard matrix A3-3

9.4

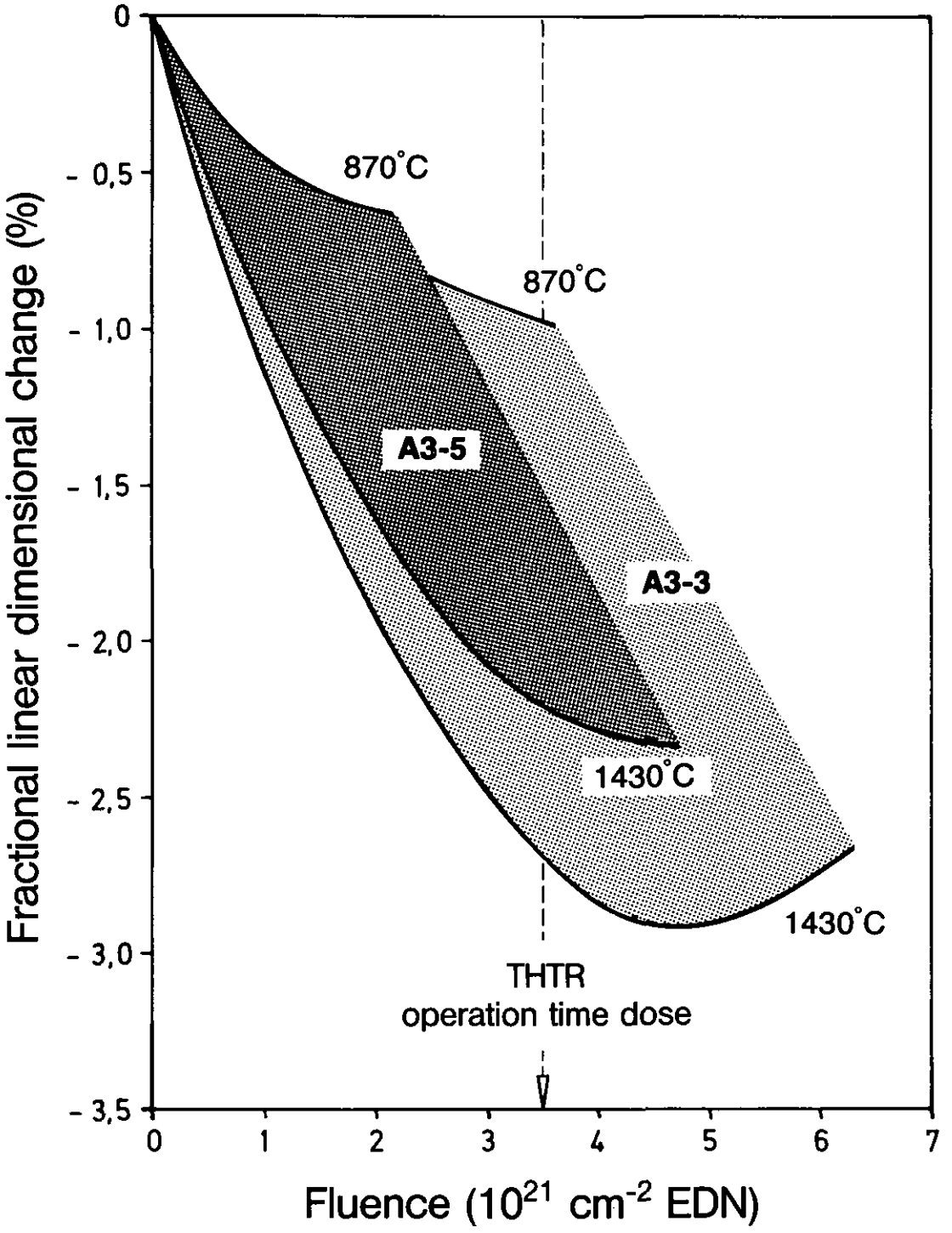

Favourable Variant
for Improvement of Strength A3-5

Comparison of the neutron-induced dimensional change with that of the standard matrix A3-3

9.5

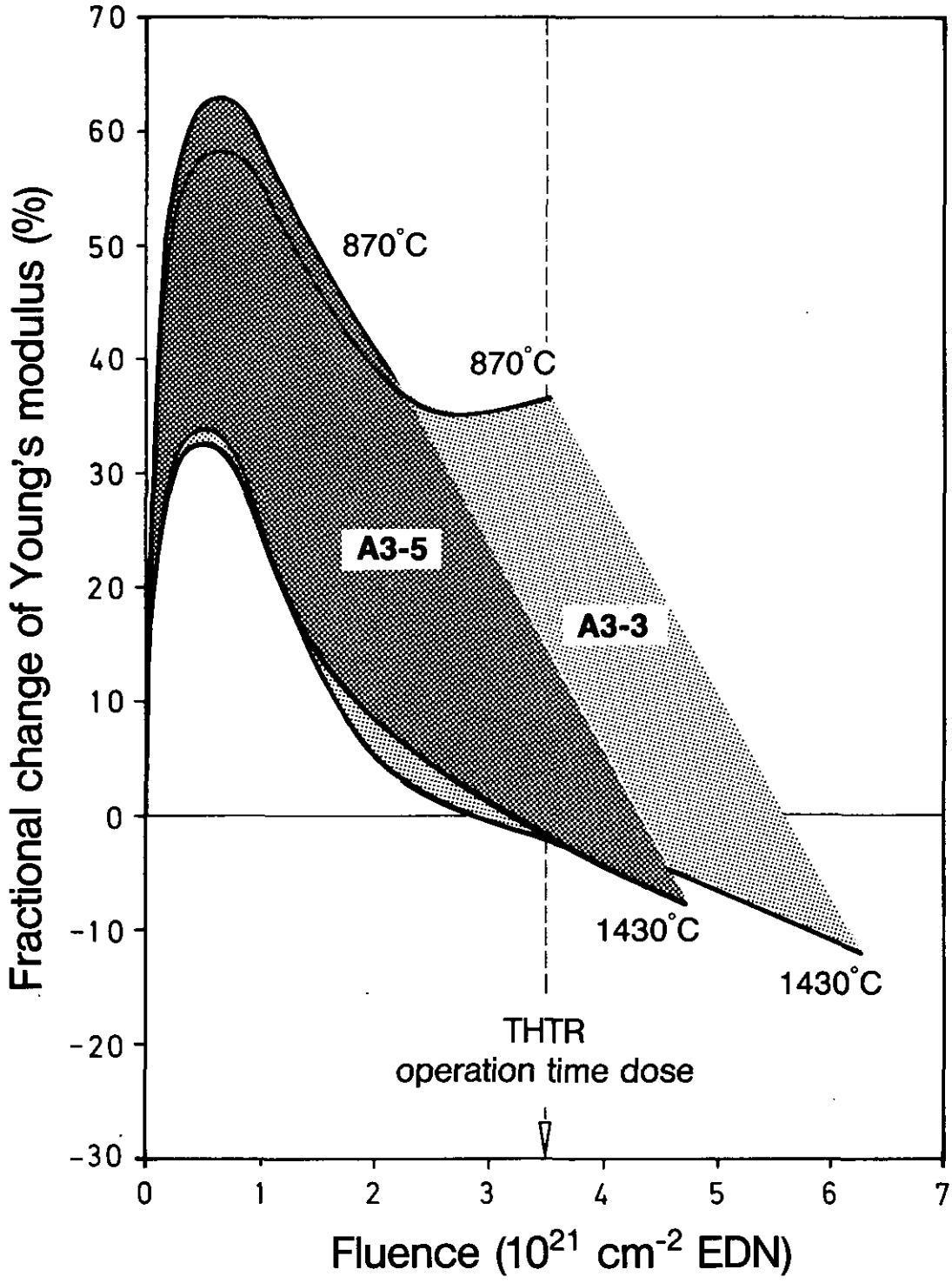

Favourable Variant
for Improvement of Strength A3-5

Comparison of the neutron-induced change of Young's modulus with that of the standard matrix A3-3

9.6

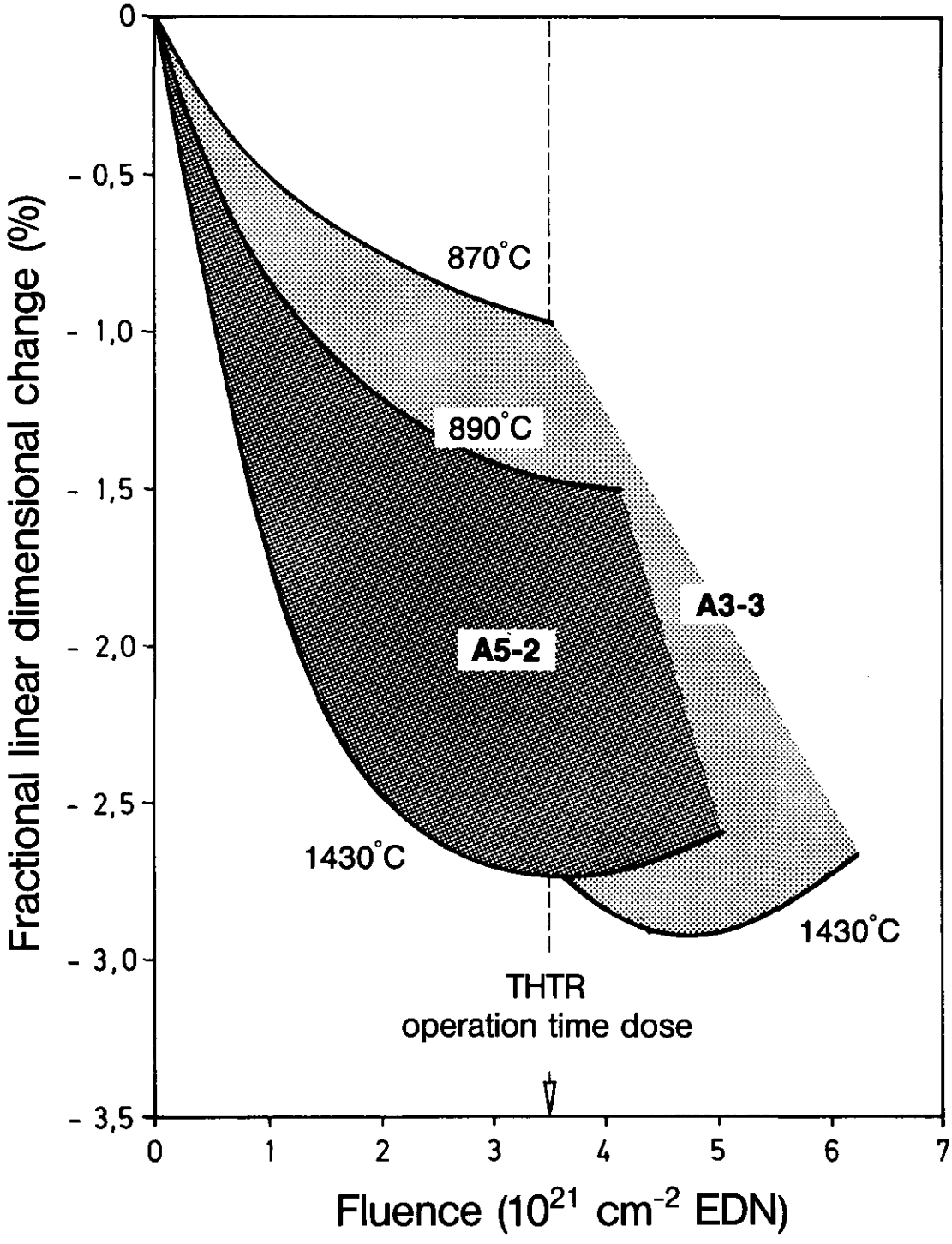

Favourable Variant
for Improvement of Strength A5-2

Comparison of the neutron-induced dimensional change with that of the standard matrix A3-3

9.7

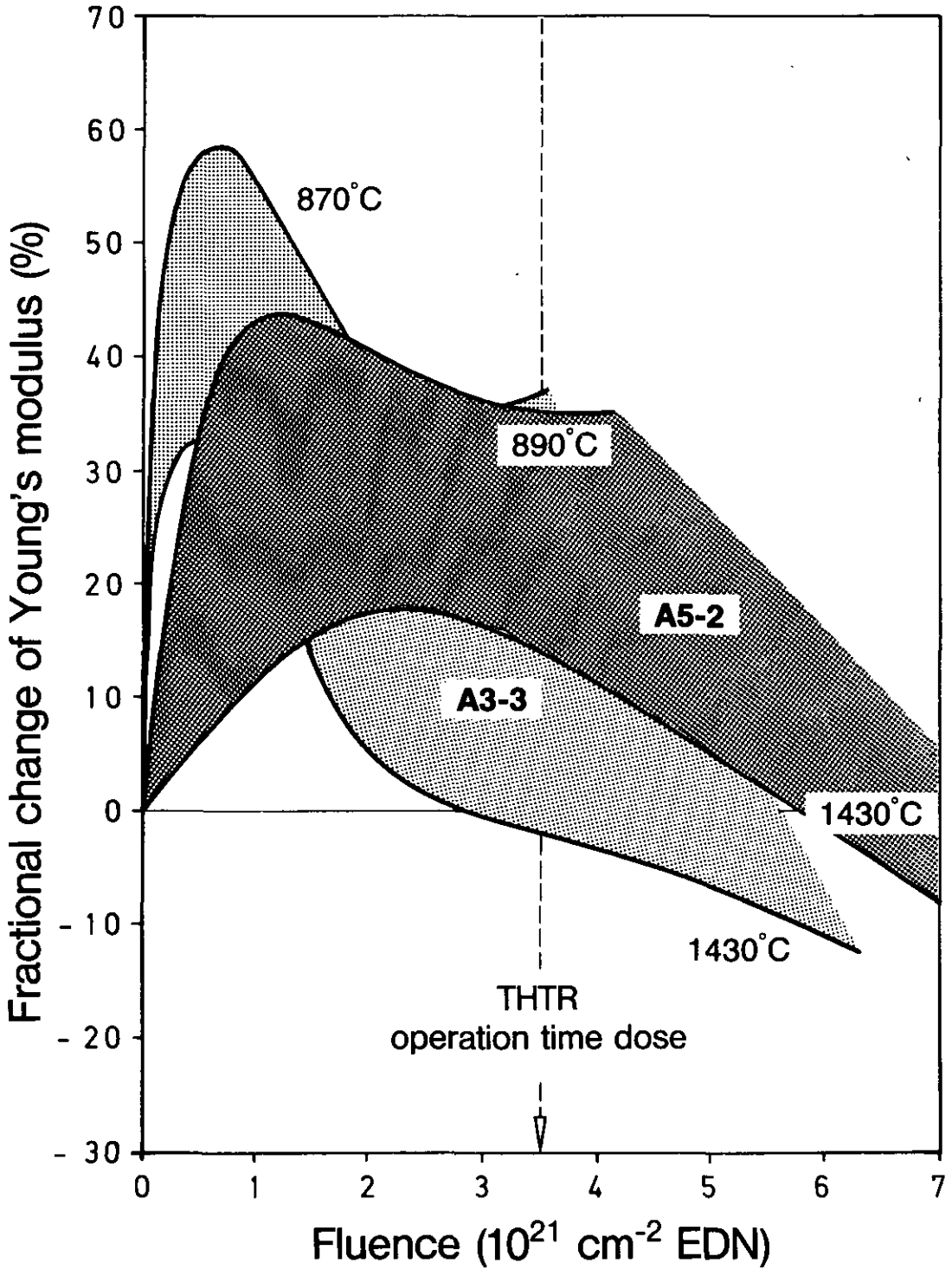

Favourable Variant
for Improvement of Strength A5-2

Comparison of the neutron-induced change of Young's modulus with that of the standard matrix A3-3

9.8

10. INFLUENCES OF IRRADIATION PARAMETERS DURING MATERIAL TESTS IN THE HFR PETTEN

- Dependence of the Dimensional Change of the Standard Matrix on Irradiation Temperature
- Influence on the Dimensional Change of the Standard Matrix Due to Differences in the Fast Neutron Flux
- Coupling of Irradiation Temperature and Fast Neutron Flux

10 Influences of Irradiation Parameters During Material Tests in the HFR Petten

The influence of irradiation parameters on the dimensional change of graphitic matrix materials will be described in the following. For this purpose, the standard matrix A3-3 is used as an example, since this material furnished the largest number of specimens for the test series so that the irradiation temperature range between 400 and 1450°C can be best supported by results.

Dependence of the Dimensional Change of the Standard Matrix on Irradiation Temperature

Figure 10.1 shows the dependence of the neutron-induced dimensional change of the standard matrix on irradiation temperature. The THTR operation time dose of 3.5×10^{21} cm^{-2} EDN was selected as a constant value for the fluence.

The isodose shows that the dimensional change, i.e. material shrinkage, is lowest at irradiation temperatures around 1000°C and increases considerably towards both lower and higher temperatures.

The general course of the isodose results form a superposition of different influences which are due to irradiation-induced processes in the material, such as

- the change in porosity,
- irradiation-induced damage to crystalline regions,
- irradiation-induced graphitization of poorly ordered regions.

Influence on the Dimensional Change of the Standard Matrix Due to Differences in the Fast Neutron Flux

Figure 10.2 illustrates how the dimensional change is influenced as a function of the fluence by differences in the flux of fast neutrons at constant irradiation temperature.

The two representations in Figure 10.2 are identical with regard to the measuring points plotted. The curve on the left shows the mean isothermal line, as is normal practice for isothermal irradiations. The clearly perceivable scattering of measured values cannot be attributed to differences in the material data prior to irradiation nor to deviations of the mean irradiation temperature, since there is an extremely good agreement in both cases.

An explanation can only be found when considering the values for the mean flux of fast neutrons. In this way, the isothermal line can be resolved to lines of constant neutron flux which hardly feature any deviations of measured values (Figure 10.2 right). It can be shown that the lower neutron flux causes a higher shrinkage of the material than the higher neutron flux.

This "flux effect" was proved not only for matrix materials, but also for other graphitic materials. Effects on various material properties were also detected in addition to those on dimensional change[2)5)11)19)20)].

Coupling of Irradiation Temperature and Fast Neutron Flux

Figure 10.3 shows the type of coupling existing between the irradiation temperature and the flux of fast neutrons during irradiation of the standard matrix in the HFR Petten. Plotted are the mean values of temperature and flux to be allocated in each case to the isothermal irradiation of the matrix specimens. The direction of specimens cut from the matrix spheres is marked by the different symbols: parallel ($\parallel$) and perpendicular ($\perp$) to the equatorial plane.

The representation shows that the flux of fast neutrons increases with the irradiation temperature. This rise is so steep in the range between 800 and 1200°C that the associated flux value at 1200°C is about 2.5 times higher than at 800°C. In the middle of this range lies the temperature flux combination for the lowest shrinkage of the material.

It may be furthermore seen from Figure 10.3 that the coupling of the two irradiation parameters is less close at low temperatures than at higher temperatures.

Corresponding couplings between temperature and neutron flux were also ob-

served during irradiation of the other matrix materials. However, fewer data were measured for the temperature-flux curves of these materials on account of the small number of irradiation specimens (cf. Figure 3.6).

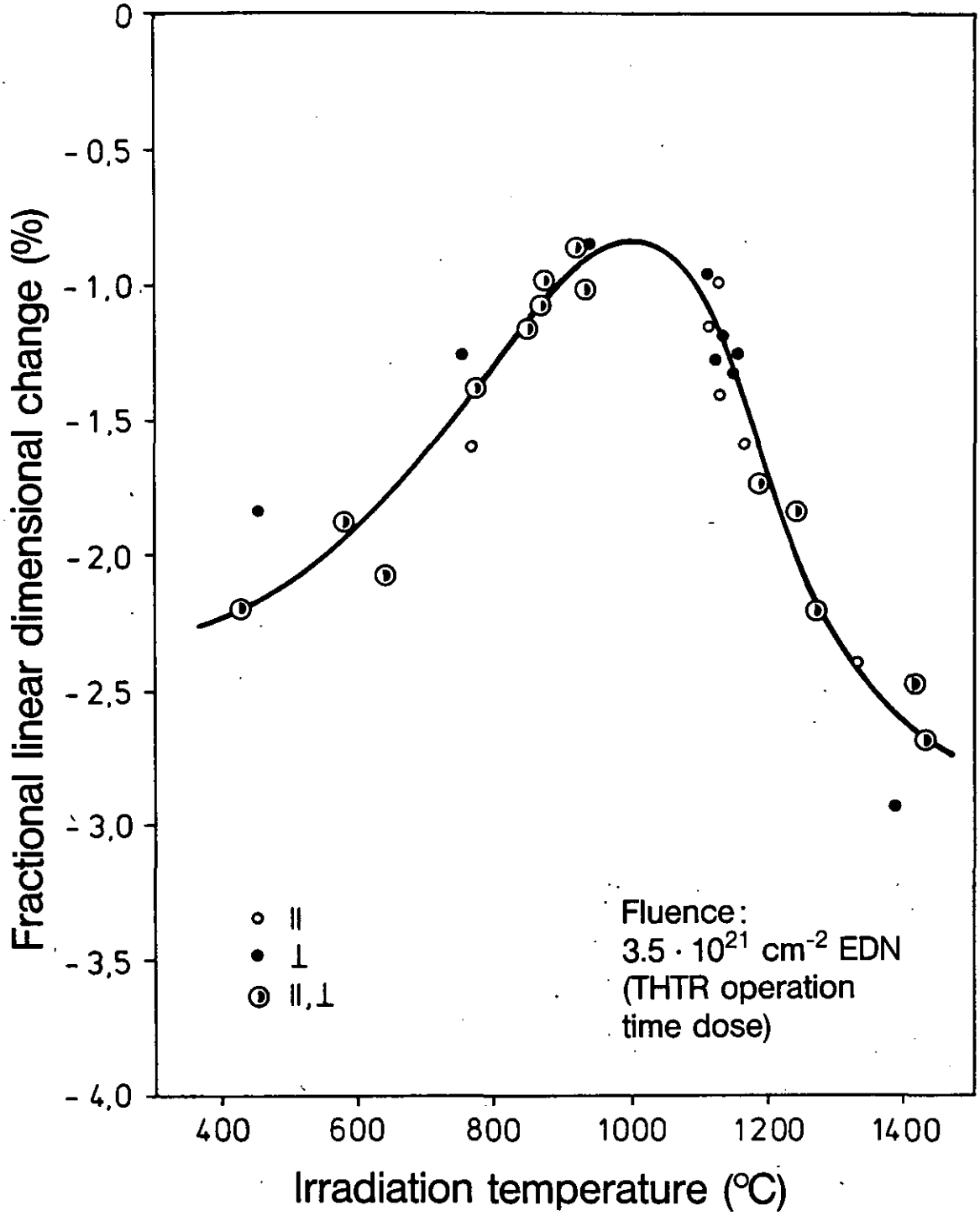

Dependence of the Neutron-Induced Dimensional Change of the Standard Matrix A3-3 on the Irradiation Temperature, shown for the THTR operation time dose

10.1

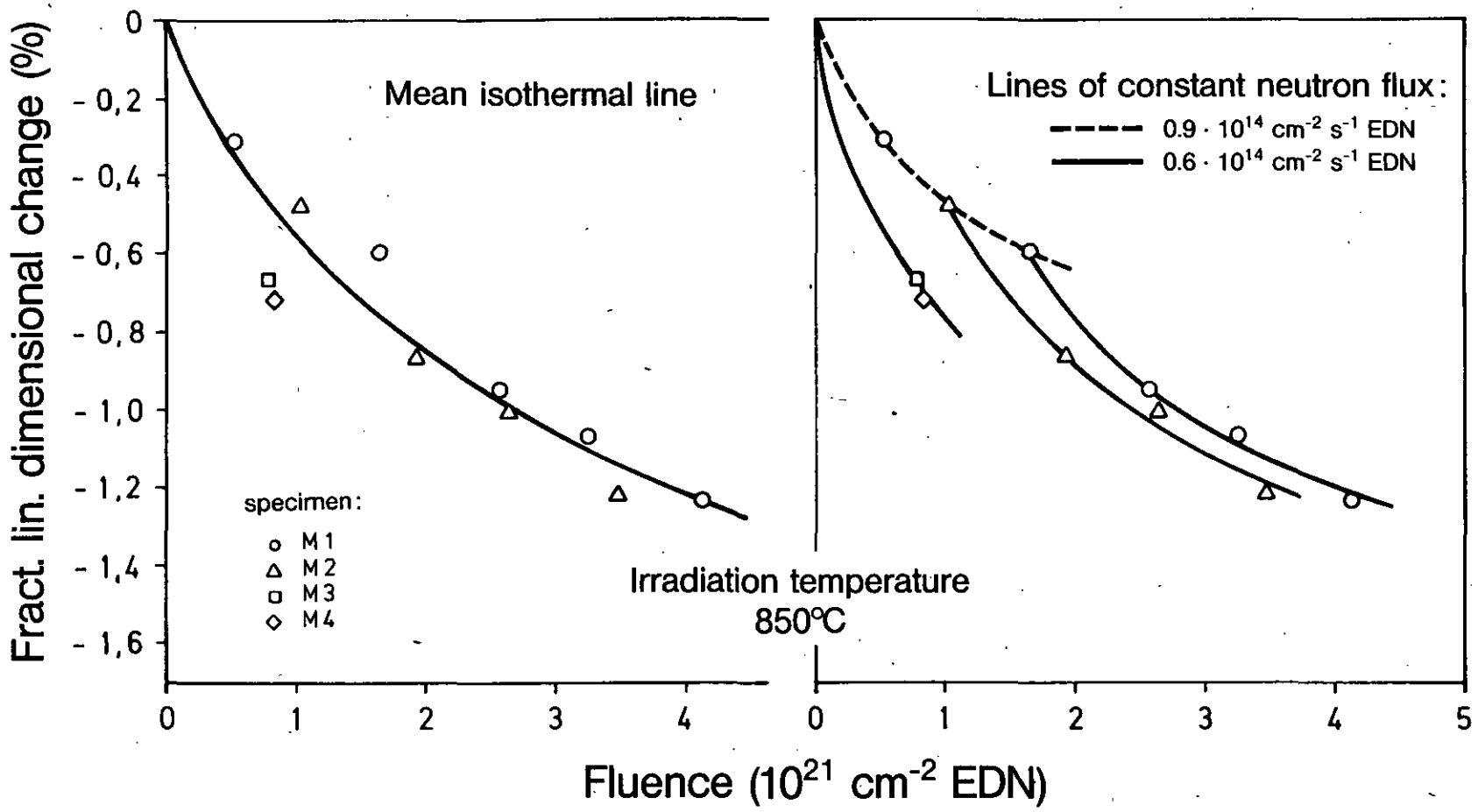

Neutron-Induced Dimensional Change of the Standard Matrix A3-3 at 850°C, Shown by the Mean Isothermal Line and the Lines of Constant Neutron Flux

10.2

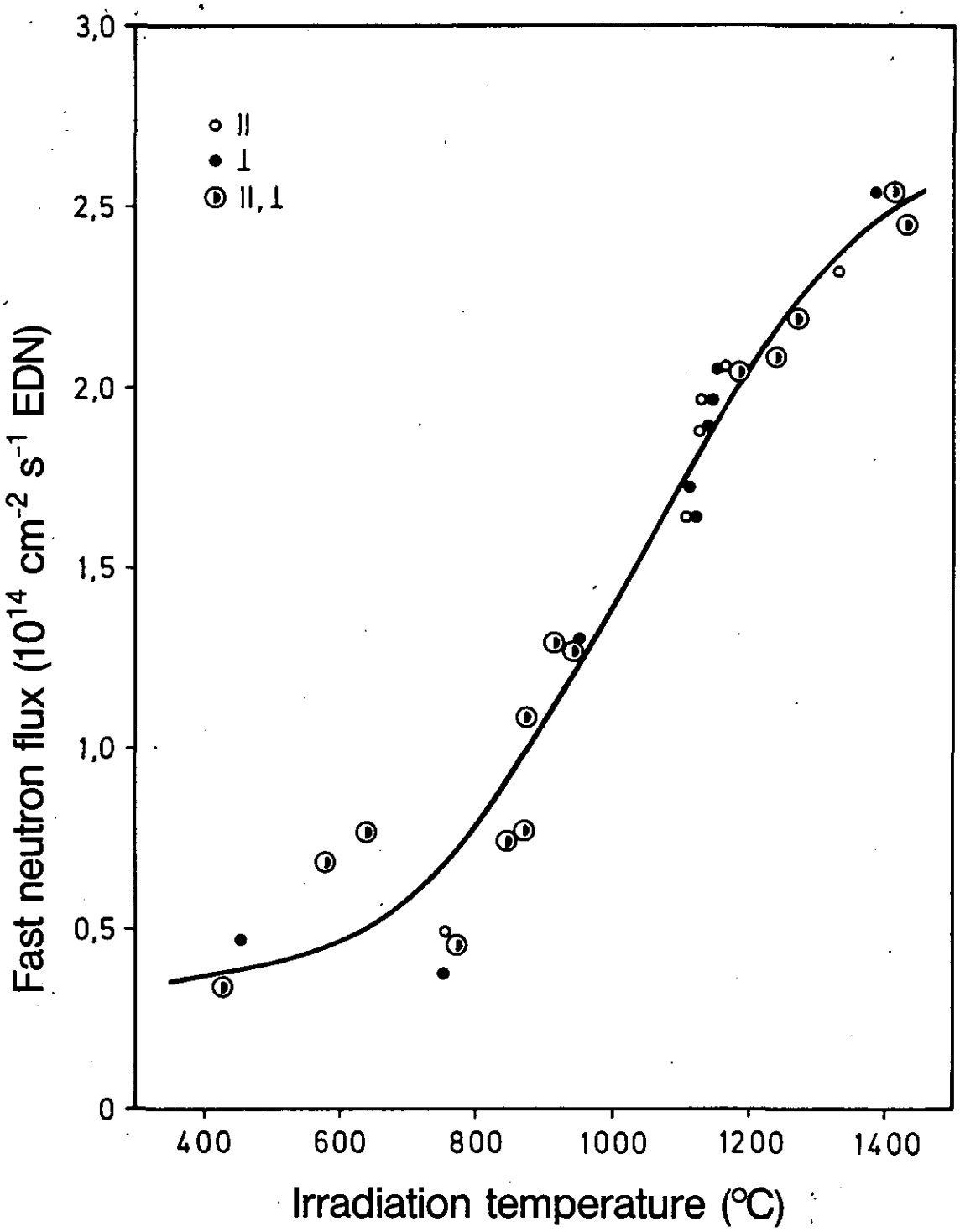

Coupling of Irradiation Temperature and Fast Neutron Flux at Neutron Exposure of the Graphitic Matrix A3-3 in the HFR-Petten

10.3

11. NEUTRON-INDUCED DIMENSIONAL CHANGE OF STANDARD MATRIX SPECIMENS IN COMPARISON WITH THE DIMENSIONAL CHANGE OF SPHERICAL FUEL ELEMENTS

- Comparative Representation

11 Neutron-Induced Dimensional Change of Standard Matrix Specimens in Comparison with the Dimensional Change of Spherical Fuel Elements

Figure 11.1 gives a comparison between the dimensional changes of specimens of the standard matrix A3-3 and those of spherical fuel elements with A3-3 as structural material. The dimensional changes as a function of the irradiation temperature of the matrix and of the surface temperature of fuel elements are plotted for the mean THTR fluence*) of 2.5 x 10^{21} cm^{-2} EDN.

The dimensional change of the standard matrix A3-3, which was determined in the isothermal material tests HFR-M13 to HFR-M32 between 400 and 1450°C in the High Flux Reactor Petten (cf. Chapters 3, 4 and 10), is illustrated by the solid curve. Regions are entered for the fuel elements irradiated in several experiments of different reactors (R2-Studsvik and DRAGON reactor). The height of these regions results from the differences of dimensional change in the direction of the polar axis of fuel element spheres and perpendicular to it. The width of the region is determined by changes in the surface temperature during irradiation.

A comparison shows that there is a relatively good agreement between the results of matrix specimens and those of fuel elements. On an average, the fuel elements of the high flux tests R2-K2 and R2-K9 in the R2-Studsvik shrinked slightly less and those of the long-time tests DR-K3 and DR-K4 in the DARGON reactor slightly more than the matrix specimens.

There are general differences between matrix specimens and fuel elements concerning the isotropy of the dimensional behaviour. While the irradiation specimens of the standard matrix behave isotropically even under strong irradiation conditions, the integral elements exhibit a lower shrinkage in the direction of the polar axis than perpendicular to it.

---

*)The mean THTR fluence is accumulated on an average by the THTR fuel elements to be transferred outwards. (The full THTR operation time dose is only reached by 10^{-4} fuel elements of the THTR.)

The anisotropic dimensional behaviour of spheres, which is attributed to the influence of the shell due to manufacture, can be seen from the height of the regions in Figure 11.1.

When discussing the dimensional change of spherical fuel elements in comparison with that of specimens of the structural material, influences due to

- fast neutron flux,
- irradiation temperature history,
- coated fuel particles

must be taken into account.

A comparison of irradiation parameters of the different experiments shows that the mean flux of fast neutrons in the fuel element tests in the R2-Studsvik was slightly higher than in the matrix tests of the corresponding temperature range in the HFR-Petten. On the other hand, the long-time irradiations of fuel elements in the DRAGON reactor, which come closer to the conditions of realistic THTR operation, showed mean flux values which were distinctly lower than those of the matrix tests.

Since the dimensional change of fuel elements is slightly smaller at higher flux values and slightly higher at lower values, it may be assumed that - in conformity with the results shown in Figure 10.2 - the influence of different neutron fluxes, possibly in connection with different neutron spectra, is effective in this case, too.

Furthermore, a different irradiation temperature history was also found for the individual experiments:

- Specimens of the standard matrix were irradiated in isothermal test series (cf. Chapters 3 and 4).
- Fuel elements of the high flux tests R2-K2 and R2-K9 in the R2-Studsvik were subjected to so-called THTR short-time cycling at surface temperatures of 600, 750 and 900°C, i.e. a frequent alternating temperature treatment. In addition, the temperature was set to 450°C during one period of irradiation in the experiment R2-K9 [21] (dotted section in Figure 11.1).

- Fuel elements of the long-time tests DR-K3 and DR-K4 in the DRAGON reactor experienced a slow temperature decrease by 200 to 250°C during irradiation of more than 700 full power days[22].

On the basis of this information about the temperature history, effects on the dimensional change of the fuel elements may be expected. As can be seen from Figure 11.1, however, these effects can only be small; probably because the experiments took place predominantly at temperatures which are at least not far from those of the shrinkage minimum of the matrix.

All the fuel elements compared contained BISO particles. The volumetric particle loading of the fuel elements was different; it amounted to 16.6 and 17.5 % in the DRAGON tests and was even below 4 % in the Studsvik tests[21]. Consequently, only minor or no influences of coated fuel particles on the neutron-induced dimensional change of the integral elements are to be expected.

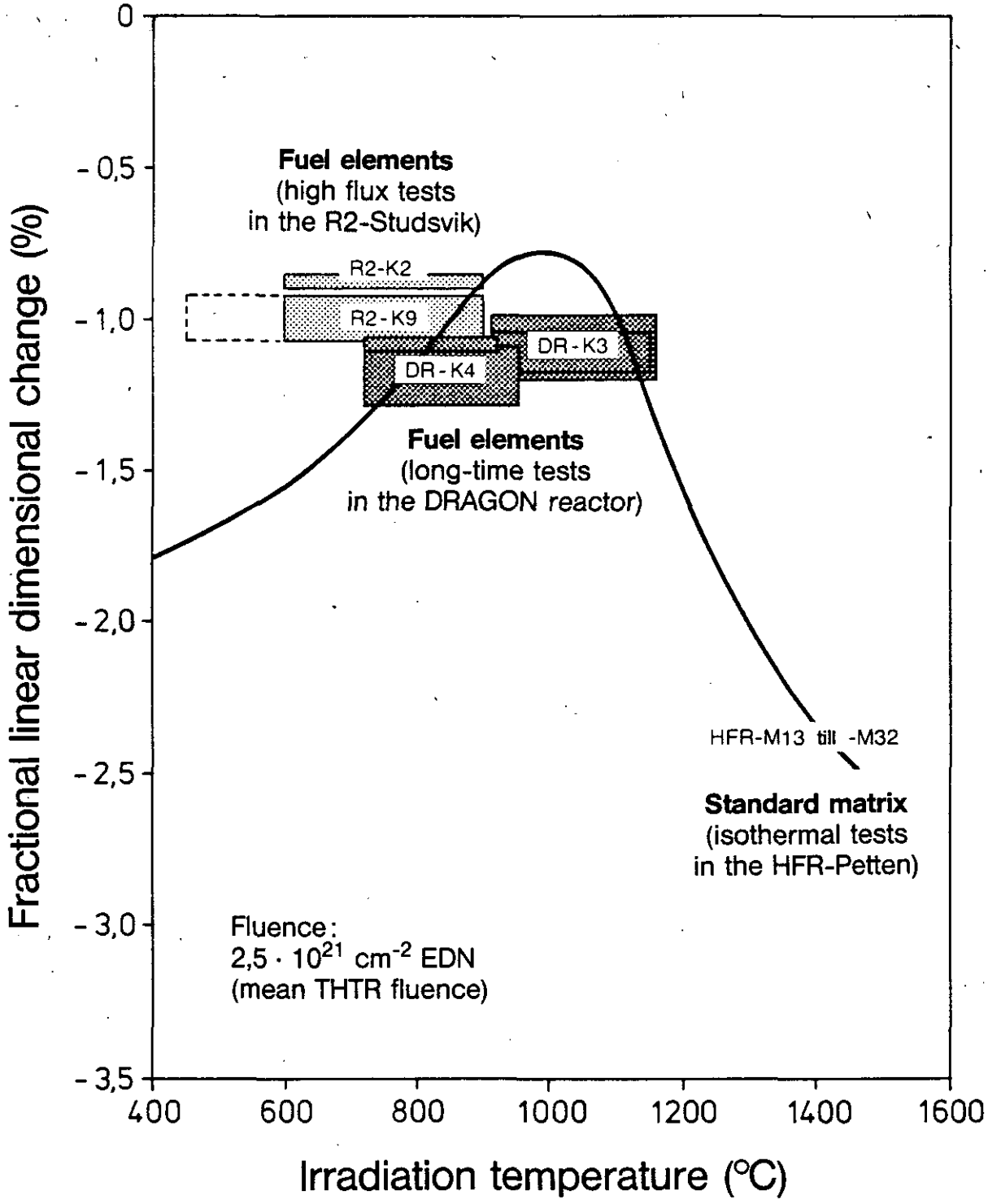

Comparisons between Dimensional Changes of the Standard Matrix A3-3 and that of Spherical Fuel Elements, Shown for the Mean THTR Fluence

11.1

12. OUTLOOK

- Warm Moulding of Spherical Fuel Elements
  - Advantages
  - Principle
- Manufacture of Matrix Powder for Warm Moulding
- Manufacture of Warm-Moulded Fuel Elements
- Warm-Moulded Graphitic Matrix Materials
  - Composition and Fabrication
  - Material Properties
  - Comparisons with the Cold-Moulded Matrix Materials A 3-3 and A 3-27

12 OUTLOOK

The development and irradiation testing of graphitic matrix materials for cold-moulded HTR fuel elements have been completed successfully with the use of two approved materials for AVR and THTR fuel elements.

Supplementary aspects result from the limits of fabricability for cold-moulded fuel elements with high heavy metal loading, on the one hand, and from efforts to further improve fabrication technology, on the other hand.

For this reason, the HOBEG company developed a process of warm moulding for spherical fuel elements. At the same time, an indigenous pitch coke graphite was used as basic raw material for the graphitic matrix instead of the raw material mixture of natural graphite and petroleum coke graphite used before.

A material test is being carried out at present in the HFR-Petten to prove the suitability of such warm-moulded matrix materials for HTR fuel elements.

Warm Moulding of Spherical Fuel Elements

The advantages which can be achieved by the warm moulding of spherical fuel elements in comparison with cold moulding are compiled in Figure 12.1.

The method of warm moulding may permit the fabrication of fuel elements even with higher heavy-metal loading than the cold- moulding process (cf. p. 25). Owing to the low moulding pressure the fracture of fuel particles during moulding is substantially lower and it appears likely to use coated fuel particles without overcoating (cf. Figure 3.3). Furthermore, remote control of the moulding operation becomes possible since the fuel elements are moulded in a steel die instead of rubber dies as before. A totally improved fabrication technology can therefore be achieved by warm moulding.

Figure 12.2 shows the principle of warm moulding for spherical fuel elements: In a steel die the ellipsoidal kernel of matrix powder and coated fuel particles, on the one hand, and the ellipsoidal shells made of matrix powder, on the other hand, are pre-moulded under the same conditions of pressure and temperature. Assembling of these pre-fabricated fuel element parts is followed by final moulding at a temperature above the melting point of the resin binder. After coking and final heat treatment the integral fuel elements are lathed

to the specified size.

Manufacture of Graphitic Matrix Powder for Warm Moulding

The manufacture of the matrix powder used for warm moulding of the fuel element kernel and the matrix shells (cf. Figures 12.2 and 12.4) is represented in Figure 12.3.

A binder solution is prepared from the basic materials phenolic formaldehyde resin and methanol and is then processed to resinated matrix powder with an isotropic artificial graphite filler (pitch coke graphite). A duroplastic binder is produced from the thermoplastic phenolic resin binder by the addition of hexamethylenetetramine as a hardener. A transition to in-situ binder synthesis analogous to the synthesized matrix A3-27 (cf. Chapters 3 and 4) seems to be possible.

Manufacture of Warm-Moulded Spherical Fuel Elements

The method developed by HOBEG for manufacturing warm-moulded fuel elements is characterized by the fact that the two-stage pressing operation is carried out in a steel die at low pressures of about 10 N x mm^{-2} and at temperatures around 100°C.

While the principle of the process is illustrated in Figure 12.2, the flow diagram in Figure 12.4 shows a breakdown into individual process steps indicating the respective parameters of temperature and pressure.

Warm-Moulded Graphitic Matrix Materials

The most important data of the two warm-moulded matrix materials W2-1 and W2-2 provided by HOBEG are compiled in Figures 12.5 and 12.6. Both materials are being tested at present under fast neutron exposure in an isothermal material test in the HFR-Petten. Variant W2-2 serves as reference material in addition to the standard quality W2-1. It exhibits a higher binder content and is intended to provide a better understanding of irradiation behaviour.

As is shown in Figure 12.5, the materials differ only by their composition, whereas the raw material and fabrication parameters are equal. The filler component consists of pitch coke graphite and the binder component has been made of prefabricated phenolic resin binder up to now to which 5 wt % of the hardener hexamethylenetetramine is added. Final heat treatment is carried out at 1950°C to achieve a favourable corrosion rate (cf. p. 75).

The material properties of the two warm-moulded matrix materials are compared in Figure 12.6. A comparison of data shows that the matrix W2-1 with the lower binder content exhibits a clearly better strength behaviour than the matrix W2-2, especially a substantially higher falling strength. Furthermore, the thermal conductivity determined at 1000°C and Young's modulus are also more favourable for this material; only the higher corrosion rate points to a slightly more unfavourable corrosion behaviour. The coefficients of linear thermal expansion determined between 20 and 500°C and, consequently, also their quotients $\alpha_\perp/\alpha_{||}$ are similar for both materials.

Figure 12.7 permits a comparison of the material properties of warm-moulded with those of cold-moulded matrix. The tabulation contains the data of the standard quality of the warm-moulded material W2-1 as well as those of the two cold-moulded materials A3-3 and A3-27 which are being used for fuel elements (cf. Chapter 4).

The three materials have different material and fabrication parameters (cf. Figures 4.1 and 12.5), but they are subjected to the same high-temperature treatment at 1950°C. The warm-moulded matrix shows a substantially better strength behaviour in comparison with the cold-moulded materials. Its values for tensile and compressive strength are between 70 and 95 % above those of the fuel element matrices and its falling strength is about 50 and 130 % higher than that of the synthesized resin matrix A3-27 and the standard matrix $A3\text{-}3_{1950^o}$, respectively. On the other hand, the thermal conductivity and, correspondingly, the electrical resistance as well as the corrosion rate are more unfavourable than for cold-moulded materials. Moreover, moulding in a die causes a higher quotient of the thermal expansion coefficients ($\alpha_\perp/\alpha_{||}$).

It is of significant technological advantage that the overcoating of coated fuel particles can probably be omitted altogether for warm-moulded fuel

elements or that at least the process flow for overcoating can be essentially simplified without the occurrence of particle fracture, especially in the case of TRISO particles with their brittle SiC layer.

Advantages of Warm Moulding Compared with Cold Moulding of Spherical Fuel Elements

Warm moulding

- enables the manufacture of fuel elements with higher heavy-metal loading
- leads to a smaller fracture of the fuel particles during fuel element moulding
- makes possible either omission or at least simplification of the overcoating procedure
- facilitates an improved technology for the manufacture of fuel elements

12.1

Viewgraph of Warm Moulding of Spherical Fuel Elements

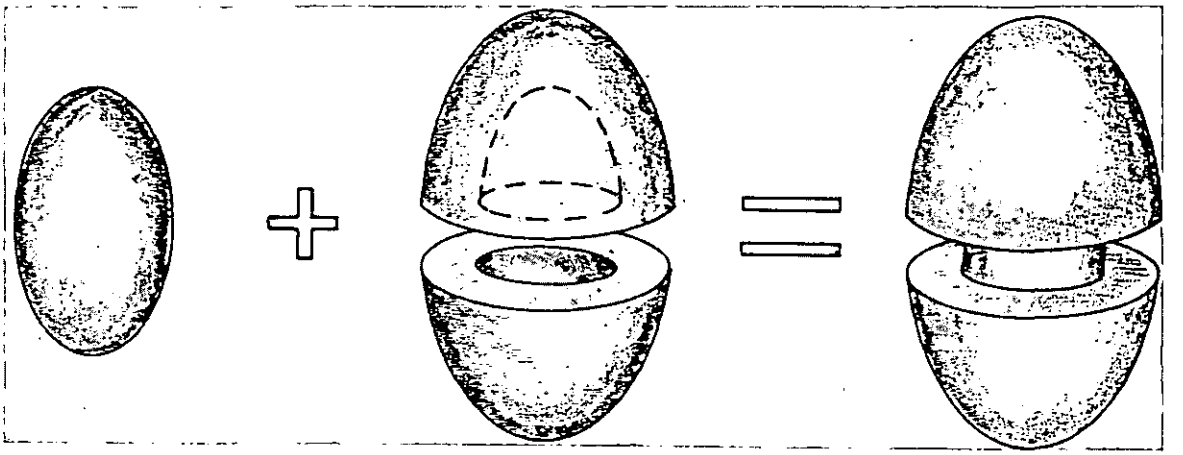

Pre-moulding of the fuel element kernel (ellipsoidal)

Pre-moulding of the matrix shells (ellipsoidal)

Assembling

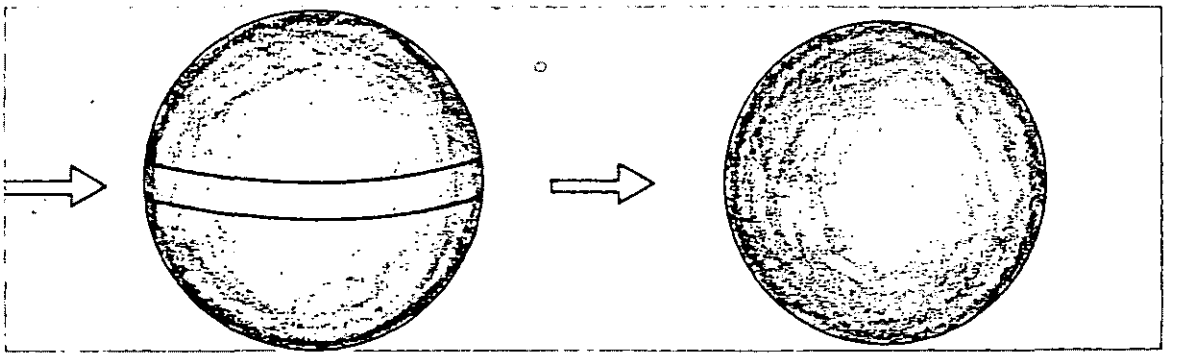

Final moulding

Heat treatment and lathing

12.2

Manufacture of Graphitic Matrix Powder for Warm Moulding

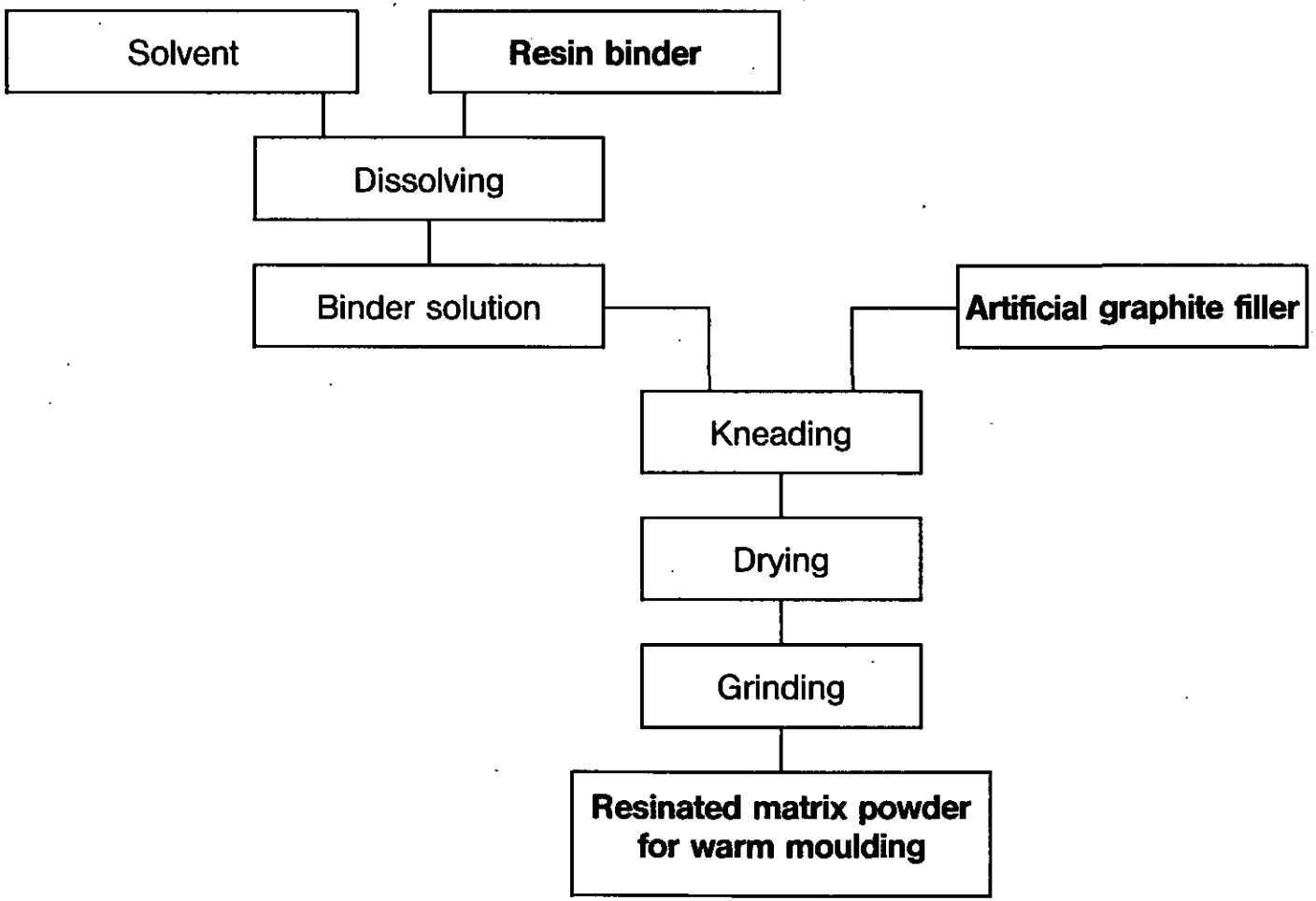

12.3

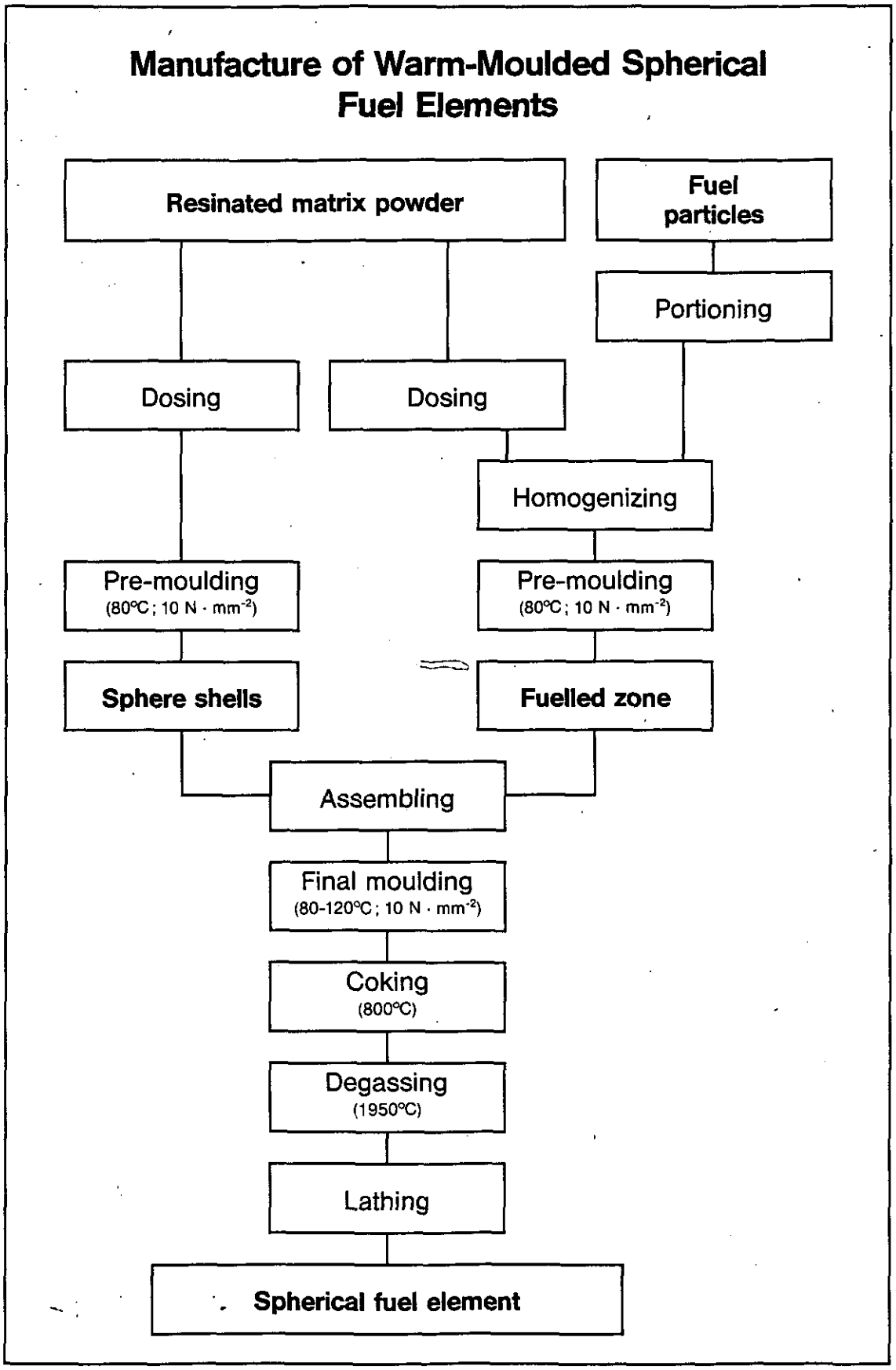
Manufacture of Warm-Moulded Spherical Fuel Elements
Resinated matrix powder
Fuel particles
Portioning
Dosing
Dosing
Homogenizing
Pre-moulding (80°C; 10 N · mm⁻²)
Pre-moulding (80°C; 10 N · mm⁻²)
Sphere shells
Fuelled zone
Assembling
Final moulding (80-120°C; 10 N · mm⁻²)
Coking (800°C)
Degassing (1950°C)
Lathing
Spherical fuel element

12.4

Composition and Fabrication of Warm-Moulded Graphitic Matrix Materials

Material and Fabrication	Warm-moulded matrix W2-1*	W2-2
Composition of raw materials: Pitch coke graphite Resin binder	 84 wt % 16 wt %	 82 wt % 18 wt %
Binder	Phenolic resin with addition of 5 wt % hardener**	
Moulding method	Warm moulding in a steel die	
High-temperature treatment	1950°C	

* standard quality

** related to the binder content

Material Properties of Warm-Moulded Graphitic Matrix Materials

Material property			Warm-moulded matrix	
			W2-1**	W2-2
Young's modulus	(kN · cm^{-2})	II*	1095	1110
		⊥*	892	980
Geometrical density	(g · cm^{-3})		1.73	1.74
Coeff. of linear therm. expansion 20 - 500°C	(10^{-6} K^{-1})	II	2.94	2.97
		⊥	3.73	3.70
Quotient of Coeff. of therm. expansion	$\alpha_\perp / \alpha_{II}$		1.27	1.25
Therm. conductivity at room temperature	(W · cm^{-1} K^{-1})	II	0.57	0.56
		⊥	0.50	0.51
Therm. conductivity at 1000°C	(W · cm^{-1} K^{-1})	II	0.35	0.30
		⊥	0.32	0.27
Spec. electrical resistance	(10^{-3} Ω · cm)	II	1.77	1.81
		⊥	2.11	2.09
Compression strength	(daN · cm^{-2})	II	844	775
		⊥	832	740
Tensile strength	(daN · cm^{-2})	II	225	132
		⊥	220	164
Falling strength Fall of a test sphere from a height of 4 m onto A3-3 spheres	(Number of falls till fracture)		1000	536
Corrosion rate at 1000°C in He of 1 bar with 1 vol. % H_2O (10 h)	(mg · cm^{-2} h^{-1})		1.14	1.01

* parallel and perpendicular to the equatorial plane of the matrix sphere
** standard quality

Material Properties of Warm-Moulded Matrix Compared with those of Cold-Moulded Matrices

Material property			Material	Warm-moulded matrix W2-1 **	Cold-moulded matrices A3-3	A3-27
			High-temperature treatment	1950°C	1950°C	1950°C
			Application	Development of warm-moulded fuel elements	AVR fuel elements THTR production	AVR fuel elements
Young's modulus	(kN · cm^{-2})	II*		1095	1000	1070
		⊥*		882	970	1020
Geometrical density	(g · cm^{-3})			1.73	1.73	1,74
Coeff. of linear therm. expansion 20 - 500°C	(10^{-6} K^{-1})	II		2.94	2.89	2.43
		⊥		3.73	3.45	2.69
Quotient of Coeff. of therm. expansion	$\alpha_\perp / \alpha_{II}$			1.27	1.19	1.11
Therm. conductivity at room temperature	(W · cm^{-1} K^{-1})	II		0.57	0.70	0.69
		⊥		0.50	0.63	0.64
Therm. conductivity at 1000°C	(W · cm^{-1} K^{-1})	II		0.35	0.41	0.44
		⊥		0.32	0.37	0.39
Spec. electrical resistance	(10^{-3} Ω · cm)	II		1.77	1.46	1.43
		⊥		2.11	1.48	1.48
Compression strength	(daN · cm^{-2})	II		844	435	469
		⊥		832	426	464
Tensile strength	(daN · cm^{-2})	II		225	135	135
		⊥		220	126	130
Falling strength Fall of a test sphere from a height of 4 m onto A3-3-spheres	(Number of falls till fracture)			1000	437	652
Corrosion rate at 1000°C in He of 1 bar with 1 vol. % H_2O (10 h)	(mg · cm^{-2} h^{-1})			1.14	0.97	0.73

* parallel and perpendicular to the equatorial plane of the matrix sphere

** standard quality

13. LITERATURE

13 LITERATURE

1) HOBEG:
Information

2) R.-E. Schulze, H.A. Schulze:
KFA-Bericht JÜL-1702, Febr. 1981

3) W. Delle, G. Haag, R. Blackstone, H. Veringa, M.R. Everett:
KFA-Bericht JÜL-1269, Febr. 1976

4) W. Delle, L. Binkele, G. Kleist, W. Rind, H.A. Schulze, R.-E. Schulze:
Jahrestagung Kerntechnik 80, Berlin, 1980, Tagungsbericht 594-597;
KFA-Bericht JÜL-Conf-38, August 1980

5) G. Kleist, H. Schiffers, H. Schuster:
Intern. Kohlenstofftagung, Carbon '80, Baden-Baden, June 1980,
preprints 565-568;
KFA-Bericht JÜL-Conf-36, May 1980

6) W. Delle, G. Haag, F.J. Herrmann, H. Luhleich, H. Nickel, R.-E. Schulze:
11th Bienn. Conf. on Carbon, Gatlinburg, 1973, Ext. Abstr. 243-244

7) H. Luhleich
Personal information

8) W. Delle, B. Heinrich, W. Heit, A. Kleine-Tebbe, W. Rind, R.-E. Schulze:
Intern. Kohlenstofftagung, Carbon '76, Baden-Baden, June 1976,
preprints 357-360;
KFA-Bericht JÜL-1316, July 1976

9) L. Binkele:
High Temp. - High Press., 4, 1972, 401

10) W. Delle, H.A. Schulze, R.-E. Schulze:
2nd Intern. Conf. on Structural Mechanics in Reactor Technology
Berlin, 1973, preprints, Vol. I, paper D 4/3

11) R.-E. Schulze, H.A. Schulze, W. Delle:
5th Intern. Conf. on Carbon and Graphite, London, Sept. 1978,
proceed. 904-917;
KFA-Bericht JÜL-Conf-25, July 1978

12) E.W. Orrell, R. Burns:
Plastics and Polymers, 36, 469, 1968

13) G.S. Learmonth, L.G. Nabi, G. Bramham, J. Bailey:
Plastics and Polymers, 37, 201, 1969

14) W. Delle, H.A. Schulze, R.-E. Schulze:
12th Bienn. Conf. on Carbon, Pittsburgh, 1975, Ext. Abstr. 127-128

15) W. Wolff; HOBEG:
Personal information

16) H.J. Becker, F.J. Herrmann; HOBEG:
Personal information

17) B.T. Kelly:
Phil. Mag., 9, 721, 1964

18) W. Delle, G. Haag, H. Nickel, H.A. Schulze, R.-E. Schulze:
4th Intern. Conf. on Carbon and Graphite, London, Sept. 1974,
proceed. 741-747;
KFA-Bericht JÜL-1128-RW, Oct. 1974

19) H.A. Schulze, R.-E. Schulze, W. Delle, A. Naoumidis:
J. Nucl. Mat. 71, 717-172, 1977

20) H.A. Schulze R.-E. Schulze, W. Delle, A. Naoumidis:
Reaktortagung des DAtF, Hannover, 1978, Tagungsbericht S. 679-682;
KFA-Bericht JÜL-1533, Sept. 1978

21) H. Ragoß:
Personal information

22) W. Burck:
Personal information